Published in final edited form as:
Adv Inorg Chem. 2016 ; 68: 1–41. doi:10.1016/bs.adioch.2015.09.001.

Opportunities and challenges for metal chemistry in molecular imaging: from gamma camera imaging to PET and multimodality imaging

Richard Southworth, **Rafael Torres Martin de Rosales**, **Levente K. Meszaros**, **Michelle T. Ma**, **Gregory E. D. Mullen**, **Gilbert Fruhwirth**, **Jennifer D. Young**, **Cinzia Imberti**, **Julia Bagunya-Torres**, **Erica Andreozzi**, and **Philip J. Blower***
King's College London, Division of Imaging Sciences and Biomedical Engineering, St Thomas' Hospital, London, UK

Abstract

The development of medical imaging is a highly multidisciplinary endeavor requiring the close cooperation of clinicians, physicists, engineers, biologists and chemists to identify capabilities, conceive challenges and solutions and apply them in the clinic. The chemistry described in this article illustrates how synergistic advances in these areas drive the technology and its applications forward, with each discipline producing innovations that in turn drive innovations in the others. The main thread running through the article is the shift from single photon radionuclide imaging towards PET, and in turn the emerging shift from PET/CT towards PET/MRI and further, combination of these with optical imaging. Chemistry to support these transitions is exemplified by building on a summary of the status quo, and recent developments, in technetium-99m chemistry for SPECT imaging, followed by a report of recent developments to support clinical application of short lived (Ga-68) and long-lived (Zr-89) positron emitting isotopes, copper isotopes for PET imaging, and combined modality imaging agents based on radiolabelled iron oxide based nanoparticles.

Keywords

radiopharmaceuticals; positron emission tomography; contrast agents; gallium; zirconium; copper; technetium

1 Introduction

Nuclear medicine is a primarily diagnostic medical imaging specialty in which tracer molecules targeted towards specific molecular processes are labeled with radioisotopes, and used to spatially and temporally map physiological and molecular processes in the body, to diagnose disease and make patient management decisions (1, 2). The use of unsealed artificial radionuclides for medical purposes in humans can be traced back to the

*senior author; Philip.Blower@kcl.ac.uk
Co-author emails: R.Southworth@kcl.ac.uk; Rafael.Torres@kcl.ac.uk; Levente.Meszaros@kcl.ac.uk; Michelle.Ma@kcl.ac.uk; Gregory.Mullen@kcl.ac.uk; Gilbert.Fruhwirth@kcl.ac.uk; Jennifer.1.young@kcl.ac.uk; Cinzia.Imberti@kcl.ac.uk; Julia.Bagunya_Torres@kcl.ac.uk; Erica.Andreozzi@kcl.ac.uk;

Europe PMC Funders Author Manuscripts

experimental use of ^{24}Na-sodium chloride by Hamilton and Stone in 1936 (3), closely followed by administration of ^{32}P-phosphate by John Lawrence in 1937-39 (3) to patients with hematological diseases and ^{131}I-iodide by Hamilton to patients with thyroid disease. Later ^{131}I-iodide became established for treating thyroid disease. However, the use of radioisotopes for diagnostic medical imaging did not become routine in hospitals until the 1970s, following the introduction of the first commercial gamma camera in 1968 (4) (and later, its evolution into single photon emission computed tomography, SPECT). Equally important in the rise of nuclear medicine was the ^{99m}Tc generator, first used for medical purposes in 1961 (4) and firmly established in routine practice by the 1970s. This simple device solved the problem of world-wide distribution of short half-life radionuclides and enabled hospitals, for the first time, to have daily access to a radionuclide with excellent imaging properties: a gamma emission spectrum with a single photopeak at 140 KeV, offering a good balance between low attenuation and efficient detection outside the body, low radiation dose to patients because of its lack of particulate emissions and short half life (6 h), and versatile chemistry. By means of the generator, ^{99}Mo, a nuclear reactor-derived beta-emitting radionuclide with a half-life of 60 h, could be transported to hospitals around the world in the form of molybdate (MoO_4^{2-}) ions bound to a solid phase (alumina). As the ^{99}Mo decays to ^{99m}Tc, the daughter product pertechnetate ($^{99m}TcO_4^-$) can be eluted from the solid phase with sterile physiological saline and converted into a variety of different tracers for a range of diagnostic applications. The range of ^{99m}Tc-radiolabelled chemical entities that quickly became accessible following the availability of the generator, combined with the ease of their synthesis on the hospital site by means of simple kits (vials containing the chemical ingredients needed to convert the ^{99m}Tc from the “raw” pertechnetate into the required chemical form) firmly established ^{99m}Tc as the most widely used radionuclide in medicine, and brought a focus on metallic radionuclides as a field in which metallochemistry could find valuable biomedical applications. Early tracers ranged from simple lipophilic complexes for hepatobiliary imaging to simple anionic hydrophilic complexes for renal function imaging, and bisphosphonate complexes for skeletal imaging.

Although the concept of positron emission tomography (PET) evolved around the same time as gamma camera imaging, it did not develop from a research tool into a widely used clinical diagnostic tool until the 1990s. Its expansion was primarily driven by the introduction of the first PET tracer of wide utility in many diseases, the glucose analog ^{18}F-fluorodeoxyglucose, (^{18}FDG), used primarily for identifying and staging cancer. While PET has the advantage of better resolution and quantification than gamma camera and SPECT imaging, the short half life of many of its tracers (e.g. only 110 min for ^{18}F) demanded significant investment in infrastructure, requiring cyclotron facilities to be installed at locations within 2-4 h travelling distance of PET scanners. The availability of the new imaging modality spawned interest in developing a much wider variety of PET tracers to enhance its versatility. This created not only applications for organic chemists to develop tracers based on small molecule metabolites and receptor ligands labeled with the positron emitters ^{18}F and ^{11}C, but also opportunities for inorganic chemists to develop novel positron-emitting metallic radionuclides (1) and to use inorganic chemistry in novel ways to incorporate ^{18}F into useful PET imaging agents (5). In this progress report, we review the use of inorganic chemistry to develop radionuclide imaging from gamma camera imaging and SPECT (with ^{99m}Tc as the

main radionuclide) towards PET (with gallium, copper, zirconium and fluorine isotopes) and multimodality imaging.

2 Technetium-99m: Small Complexes

2.1 From serendipity to design

The ^{99m}Tc-labelled radiopharmaceuticals that came into widespread daily use in the 1970s were largely a product of early biological experiments in which complexes were made with "off the shelf" chelating ligands selected in the absence of detailed knowledge of the coordination chemistry of technetium (1). In most cases their structures remain unknown even now, and their approval in today's regulatory climate would have been most unlikely. Nevertheless they were extremely successful and medically useful. Examples (Fig. 1) include DTPA (**1**), *meso*-DMSA (**2**), bisphosphonates (**3**), HIDA (**4**), and various colloids (predating "nanotechnology" by decades) and macroaggregates made from albumin.

In the 1980s and 1990s, as understanding of the coordination chemistry of technetium grew (6), a new generation of complexes found their way into nuclear medicine, with a greater element of chemical design in their development and with well-defined structures but still with simple, kit-based synthesis. It became clear that because of the greater covalent character and greater pi-bonding tendency (both ligand-to-metal and metal-to-ligand, depending on oxidation state) shown by technetium compared to other metals discussed in this article, polydentate chelators were not always necessary and bidentate and even monodentate ligands would provide sufficient *in vivo* kinetic stability for many purposes (1). The concept of technetium "cores" emerged – that is, a set of well-defined stable complex building blocks adapted to the coordination preferences of technetium (and in most cases, importantly, to rhenium too) that could be elaborated and functionalized for different purposes. Examples (Fig. 2) include the TcO^{3+} (with mixed tetradentate sulfur and nitrogen chelating ligands such as the MAG3 complex (**5**) for renal function imaging, "pentavalent" DMSA complex (**6**) for medullary thyroid carcinoma and bone disease (7–15), HMPAO complex for cerebral perfusion imaging and cell labeling (**7**), $Tc(isonitrile)_6^+$ (**8**, e.g. sestamibi for myocardial perfusion imaging), TcO_2^+ (with tetraamine **9** or diphosphine **10** chelating ligands), $Tc(CO)_3^+$ (**11**) and $TcN(dithiocarbamate)_2$ (**12**) (16–20). Some of these are discussed in more detail below.

2.2 Tc(I)tricarbonyl

The Tc(I) tricarbonyl core offers exceptional kinetic stability, especially when incorporated into complexes in which it is attached to targeting ligands by means of a bifunctional chelator designed specifically to accommodate the low oxidation state technetium (i.e. tridentate and able to coordinate in a facial geometry (**11**, Fig. 2) (21). A number of ligands have been devised for the latter approach, including the dipyridylamino (dpa) group in which the chelator is incorporated into an amino acid ready for incorporation into a peptide using solid phase synthesis,(22) as described below for hynic. The dpa chelator has been used to link $^{99m}Tc(CO)_3^+$ not only to biomolecules but to small molecule targeting moieties such as bisphosphonate derivatives (**13**, Fig. 3) (16–20). This offers a potential advantage over conventional technetium bisphosphonate complexes, because the bisphosphonate group

is free and available to fulfill its biological function (e.g. binding to bone mineral) rather than being partially protected by binding to the technetium, and because the structure of the complex is known, homogeneous, well-defined and stable, in contrast to the mixtures of unstable complexes obtained with conventional bisphosphonates in ^{99m}Tc-labelling kits. The result is higher and more prolonged incorporation into regions of high bone turnover, despite their slower kinetics (19, 20). These complexes can also be used for imaging soft tissue and vascular calcification (16) and for linking ^{99m}Tc to various inorganic nanoparticulate materials (such as iron oxides) for combined modality imaging (17, 18, 23).

2.3 Tc(V) complexes

There is an extensive literature, which is beyond the scope of this article, describing Tc(V) mono-oxo-complexes with linear tetradentate chelators containing a combination of sulfur and nitrogen ligands: N4 (24, 25), SN3 (**5**, Fig. 2), and S2N2 (where S is thiolate or thioether (26) and N is an uncharged amine or a deprotonated amine or amide) (27). In addition, the Tc(V)-oxo-bis(dithiolate) core, best known in the form of the dimercaptosuccinic acid complex (**6**, Fig. 2) (8, 9), is notable for its excellent *in vivo* stability (11) well-defined structure and ease of synthesis under mild conditions directly from pertechnetate. This complex is useful clinically for imaging of medullary thyroid carcinoma (28) and metastatic bone disease (11, 12) and other tumors. It also has potential for conjugation to targeting ligands by virtue of its carboxyl groups. The synthesis of the corresponding dianhydride of this complex (15) provides a simple route to functionalization by reaction with amines linked to targeting groups such as phosphonate (29), imidazole (30) and biomolecules (15), while esterification of the complex offers further opportunity for biological targeting. Despite its advantages of ease of synthesis, well-defined structure and biological stability, it suffers from the limitation that, having two separate bidentate ligands, it forms three isomers (*syn-endo*, as shown in Fig. 2, *syn-exo*, and *anti*), making this system less attractive from a regulatory standpoint. Once one or more of the carboxylate groups is conjugated, the number of isomers increases further. In the case of the rhenium analogue, some progress in improving the preference for a single isomer (*syn-endo*) (15) has been made by judicious choice of synthesis conditions and reducing agent, but this remains a challenge for further development in the case of ^{99m}Tc.

The Tc(V)-nitrido core, which is also well-characterized structurally in the form of bis(dithiocarbamate) complexes, has become recognized recently as a means of synthesizing structurally well-defined complexes (31) such as the myocardial perfusion imaging agent ^{99m}Tc-NOET (**12**, Fig. 2) (32), taking advantage of its ability to act as a center for assembly of two targeting ligands (such as antibiotics, bisphosphonates (16)), and thus offering a platform for synthesis of “divalent” targeting agents. Although the divalent bisphosphonate derivatives (**14**, Fig. 3) provide excellent SPECT images of bone remodeling and soft tissue and arterial calcification (16), the extent to which their divalent nature is advantageous for this class of complexes is not yet clear, although divalency has been established as a successful approach to enhancing target affinity in other bioconjugate systems (33). The high symmetry of these complexes, and the fluxionality of the coordination sphere, means that the isomerism that besets the dimercaptosuccinic acid system may be less problematic in the dithiocarbamate ligand system. However, it does not have the advantage of being

easily synthesized in a single step from pertechnetate: the current method requires synthesis of the Tc(V) nitride core with intermediate ligands prior to a ligand substitution step. This system will have much greater promise if a single step synthesis can be devised.

2.4 Bioconjugates: a new challenge

Following the development of well-characterized small complexes based on stable technetium core complexes, the design of molecular imaging agents has shifted again, towards targeting specific receptors and transporters, by incorporating ^{99m}Tc into biomolecules such as peptides and proteins (1). The “technetium core” principle has been important in this endeavor. Although the synthesis of ^{99m}Tc-radiopharmaceuticals as simply as possible using minimal equipment remains an important aspiration to increase their likelihood of clinical application, the development of simple labeling kits for the new generation of biomolecular tracers has had limited success.

It is outside the scope of this review to catalogue the various approaches to synthesis of ^{99m}Tc bioconjugates; instead it is appropriate to identify the challenges that remain in achieving the “one-step” kit-based ideal. The chemistry is complex, as most approaches entail both exchange of ligands and reduction of Tc(VII) in order to convert pertechnetate into the bioconjugate, and the process must proceed quickly, using non-toxic reagents, under mild aqueous conditions, in almost quantitative yield to avoid the need for purification which introduces undesirable additional steps. The closest approach to this ideal is represented by the examples of a bifunctional chelator, hydrazinonicotinamide (hynic) (34) and the tricarbonyl ($Tc(CO)_3^+$) complexes.

2.5 Bioconjugation with hynic

Hynic (**15**, Fig. 4) can be conjugated to targeting molecules via its carboxyl group, and the hydrazinopyridine group offers a potentially bidentate coordination of technetium with the coordination sphere completed by a range of other monodentate and chelating ligands. Hynic is widely used to label proteins and peptides with ^{99m}Tc, and the bioconjugation is often depicted as incorporating a monodentate coordination to technetium via the hydrazine functionality. However, comparison of the coordination behavior of relatives of hynic **16**-**20** shown in Fig. 4 and with phenylhydrazine analogues, X-ray crystal structures of model complexes and mass spectrometry of the technetium complexes (35, 36) using the long-lived isotope 99Tc suggests otherwise: bidentate coordination, via both the terminal nitrogen of the hydrazine moiety and the pyridine nitrogen, is more likely (**21**, Fig. 4), with technetium formally in oxidation state V and free of oxo, hydroxo and chloride ligands. The kinetic stability of the Tc-hynic coordination is adequate to survive *in vivo* conditions. The kinetics of radiolabelling of hynic conjugates, using raw pertechnetate and with stannous chloride as a reducing agent, can be excellent and conducive to the ideal of kit-based labelling at high specific activity and without need for post-labeling purification. However, this efficiency varies greatly among different co-ligands used to complete the coordination sphere of the technetium atom. Reduction of pertechnetate by stannous chloride in the presence of tricine provides excellent labeling efficiency, but the ternary complex formed has multiple coordination isomers with tricine coordinated in different modes, and is vulnerable to ligand exchange under *in vivo* conditions, including the possibility that histidine side chains near

the hynic-containing residue contribute to the technetium coordination sphere (36)(37). Ethylenediaminediacetic acid (edda) does not create ideal labeling conditions when used in this way but provides greater stability and fewer isomers (**21**, Fig. 4 (37). The advantages of both can be gained by performing the initial labeling using tricine and then substituting edda, but this creates an additional step and does not completely solve the problem of isomerism. The ideal kinetics created by tricine probably arise because the intermediate Tc(V)-oxo-tricine complex formed upon reduction of pertechnetate in the presence of tricine is, fortuitously, close to optimal for reaction with hynic in a way that edda and other ligands cannot match. Since mechanistic details of this multi-step redox/ligand substitution reaction are unknown and inevitably very complex, it is hard to predict what types of ligands will provide the desired combination of fast kinetics of complexation, high resistance to transchelation *in vivo*, and formation of a single isomer. The combination of hynic and tricine provides a starting point for this search; a number of alternative co-ligands based on phosphines and pyridine derivatives have been evaluated but an optimal design has not yet been reached (34). Nevertheless, synthetic refinements to facilitate easy use of hynic for ^{99m}Tc labeling of peptides and proteins have been developed, including derivatives with the carboxyl linker group in different position (Fig. 4) (38), hynic-amino acid derivatives to incorporate hynic into peptides site-specifically using conventional solid-phase synthesis (39), conjugates with maleimide and other linkers to increase versatility of linkage to proteins, and protected forms of hynic (40, 41) to prevent cross reaction of the reactive hydrazine moiety with proteins and peptides. The protected forms include a trifluoroacetyl derivative in which the complex formation with technetium catalyzes the deprotection (42), ensuring that free reactive hydrazine groups are not exposed at any point pre- or post-labeling.

2.6 Bioconjugation with other bifunctional chelators

Some of the Tc(V) cores with nitrogen and sulfur ligands described above have demonstrated potential as bifunctional chelators for biomolecule labeling. The most readily accessible (by virtue of the commercial availability of kits for MAG3 labeling) is **5** (Fig. 2) (43), which can be linked to proteins and peptides by activation of its uncoordinated carboxyl group. The DMSA anhydride complex of rhenium (15) mentioned above suggests a possible route to developing analogous technetium chemistry as a biomolecule labeling system. A novel approach in which two DMSA moieties are bridged by a linker to produce a tetradentate bifunctional chelator has the potential to simplify the use of the DMSA system for bioconjugation (44).

2.7 Bioconjugation with the “Tricarbonyl core” $Tc(CO)_3^+$

The $Tc(CO)_3^+$ core is an extremely versatile synthon that can be incorporated into targeting agents not only in the form of small molecules, as described above, but also as a direct attachment to proteins via polyhistidine sequences (His-tags, sequences of typically six histidine residues), offering excellent kinetic stability of the final labeled product (45). Because many bioengineered proteins incorporate His-tags, this is particularly convenient and provides a degree of site-specificity because the ^{99m}Tc becomes attached much more efficiently to the His-tag than to other amino acid sequences (46). Until recently this site specificity was assumed rather than proven, but analysis by tryptic digest and electrospray

mass spectrometry has shown that although a single histidine residue is sufficient to incorporate the ^{99m}Tc, the labeling is indeed selective for the His-tag(47, 48). The structural details of the facial coordination of the $^{99m}Tc(CO)_3^+$ fragment by the protein, including the identity of the donor atoms and the number of histidine side chains involved, remain unknown, and it is likely that isomers are formed leading to inhomogeneity of structure. There are certainly variations in labeling efficiency between proteins: some can be labeled efficiently at low concentration while others require purification even after labeling at relatively high concentration, indicating that the identity of the amino acids in the vicinity of the His-tag, and perhaps the overall protein structure, influence labeling efficiency. In particular, incorporation of a nearby cysteine residue (47–49), or modification of the protein to incorporate a thiol prosthetic group (50), improved the labeling efficiency under mild conditions. To help identify the factors affecting labeling efficiency, and to engineer an optimal His-tag design that would ensure efficient labeling of any protein containing the sequence, a high-throughput screen approach was adopted in which various arrangements of His-tag sequences and accompanying amino acids were screened for ^{99m}Tc labeling on a solid-supported two-dimensional array. This screen showed that labeling efficiency could be enhanced by an order of magnitude, under mild conditions (room temperature, neutral pH, very low protein concentration) by including positively charged amino acids close to the His-tag, if the labeling is performed in the conventional phosphate buffer (Fig. 5) (51, 52). This raises the possibility of designing targeting proteins not only to bind to their target receptor but also to ensure the simplest and most efficient labeling and avoid the need for purification steps.

Despite these advances, the $^{99m}Tc(CO)_3^+$ fragment remains sub-optimal for routine use in hospitals because it is necessarily a two-step process – first the $^{99m}Tc(CO)_3^+$ fragment has to be synthesized (and sometimes purified) and then it has to be incubated with the protein. Although conditions have been optimized to make the labeling as simple and efficient as possible (49), the challenge to achieve single-site labeling in a single step under mild conditions to give a homogeneous, high specific-activity product remains unmet.

2.8 Bioconjugation by direct labeling via cysteine

A well-established route to incorporating ^{99m}Tc into monoclonal antibodies is reduction of inter-chain disulfide (cystine) linkages followed by insertion of pre-reduced ^{99m}Tc by ligand substitution, to take advantage of the affinity of ^{99m}Tc for thiolate ligands. This is a simple and reliable method, with wide utility and versatility, but the labeled antibody has limited *in vivo* stability compared to antibodies labeled with (for example) ^{111}In via well-designed chelators such as DTPA and DOTA derivatives. There have been a number of attempts to use a similar approach to label smaller peptides containing cysteine loops; however, the labelled products are usually poorly characterized with unknown structures. The only attempts to define structurally the complexes formed (using electrospray mass spectrometry) have entailed use of water-soluble phosphines as the reducing agent for the disulfide bond, and have shown mixtures of species with poor stability, incorporating phosphine as well as thiolate in the coordination sphere, and ^{99m}Tc in oxidation state III (53). The lack of structural control makes this method quite unsuitable for labeling of peptides and smaller proteins.

2.9 Rhenium analogues

The potential importance of radionuclide therapy with beta-emitting isotopes ^{186}Re (half-life 90 h, β^-, γ) and ^{188}Re (half-life 17 h, β^-, γ(54)) makes the periodic relationship between rhenium and technetium of great interest. The early chelating systems used before the recognition of the important stable technetium cores were not readily amenable to the inference of structural and biological parallel between technetium and rhenium, and many attempts to recreate $^{186/188}$Re-labelled complexes of this type have been unsuccessful (notably, for example, the rhenium and technetium complexes with coordinated bisphosphonate ligands have completely different biological behavior and stability (19, 20, 27, 55)). However, when the stable core systems are used there is much greater parallel between rhenium and technetium, and much of the chemistry can be applicable to both metals, albeit often with adjustments to the labeling conditions to take into account the typically reduced reactivity, and reduced tendency towards reduction to lower oxidation states of rhenium compared to technetium. The $M(CO)_3^+$ systems show close structural analogy, as demonstrated by the dpa-bisphosphonate conjugate complexes (19, 20) and the labeling of proteins with his-tags; the preferred his-tag-based amino acid sequences identified as most efficient for ^{99m}Tc were also optimal for ^{188}Re (52). The pentavalent ^{99m}Tc and 188Re dimercaptosuccinic acid complexes also show identical structure (7–10) and (human) biological (13, 14) behavior, as do the dithiocarbamate-bisphosphonate conjugates (16).

2.10 Summary: challenges in Tc-99m chemistry

The early development of ^{99m}Tc radiopharmaceuticals was characterized by very simple preparative methods that disguised extremely complex coordination chemistry. As technetium coordination chemistry became better understood, more stable and well-characterized complexes entered the clinical arena, with labeling methodologies remaining relatively simple. In the age of molecular imaging with bioconjugates (proteins, peptides etc.), however, the methodology for radiolabelling has become more complex, which has hampered the widespread clinical use of labeled biomolecules. The chemistry of technetium is among the most complex of any element and the challenge to produce labeled bioconjugates with homogeneous structure, under mild conditions, in a single step, at low concentration/high specific activity is a goal that has not been met and deserves renewed effort. The recent shortages of ^{99}Mo and hence ^{99m}Tc, resulting from planned and unplanned downtime of nuclear reactors, has highlighted the global fragility of ^{99m}Tc supply (56). The current international effort to plan new reactors, and develop new generator and elution designs to cope with lower specific activity ^{99}Mo (57) and alternative cyclotron-based means of production, testifies to the future continued importance of ^{99m}Tc and encourages renewed efforts to develop technetium chemistry to achieve these goals.

3 The transition towards PET

3.1 The need for metallic positron emitters

Despite the clinical success and wide availability of gamma camera and SPECT imaging, and its advantages of relatively low cost and capability for imaging two or more isotopes simultaneously, the superior resolution and quantification of PET has made it increasingly

more attractive even for applications that do not require organic small molecules like ^{18}F-FDG. This has created opportunities for new chemistry to incorporate positron-emitting metallic radionuclides into radiopharmaceuticals. Foremost among these are ^{68}Ga, ^{89}Zr and the copper isotopes $^{60/61/62/64}$Cu.

3.2 Gallium-68: “the new technetium-99m”

In many ways ^{68}Ga (half-life 68 min) is emerging as “the new technetium,” i.e. a short half-life metallic radionuclide produced from a generator and easily introduced into a variety of molecules and biomolecules, but for PET instead of single photon imaging. It is produced on the hospital site by decay of germanium-68 (half-life 271 days) via the ^{68}Ge/^{68}Ga generator (58). The decay of ^{68}Ga produces a high yield of positrons and the Ga^{3+} eluted is readily chelated with a variety of chelating agents (59) with good kinetic stability. Despite growing clinical use in recent years, especially in Europe, only in 2014 was the first commercial generator given marketing authorization for clinical use. This development has led to rapid expansion of its use. Its chemistry is much simpler than that of technetium, and there is only one relevant oxidation state (III). Nevertheless the chelating agents used to couple it to biomolecules explored to date (**22**-**27**, Fig. 5) have not been conducive to simple application in hospitals with limited radiochemistry facilities, requiring multiple operations including heating, use of low pH and purification steps. A genuinely single-step, kit-based labeling procedure that is functional at room temperature, moderate pH and very low concentration, affording a complex with good *in vivo* stability, would greatly increase its attractiveness and accessibility to more hospitals and patients. The current generation of chelating agents, mostly based on macrocyclic polyaminocarboxylate designs (Fig. 5), meet some but not all of these requirements. Considerable effort has been focused recently on developing new chelators to overcome these problems. Much of the recent work has been summarized in an excellent recent review and is beyond the scope of this article (59).

In our laboratory, the approach to meeting these needs is to move away from macrocyclic ligands, and to exploit the similarity in coordination behavior of Ga^{3+} with that of Fe^{3+}. This has led us to the design of tripodal tris(hydroxypyridinone) (THP) ligands (60) that incorporate iron-chelating side arms based on the successful iron-chelating drug Deferiprone (**28**, Fig. 5) (61). The resulting chelating systems **29**-**32** form gallium complexes very rapidly at very low concentration, room temperature and neutral pH; only a single complex species was detected by HPLC, with a 1:1 stoichiometry as determined by electrospray mass spectrometry. The ^{68}Ga complex of **29** has a very high association constant (logK = 29.1 (62)) and excellent *in vivo* stability, and thus meets the requirements listed above more completely than other ligand designs recently reported (59). Direct comparison between chelators was investigated by progressively reducing the chelator concentration until labeling efficiencies began to fall below 95%, based on the premise that any chelator will efficiently complex the metal if its concentration is high enough; the best ligands will therefore retain efficiency at the lowest concentrations. With this approach we showed that THP-Ac (**29**, Fig. 5) outperformed established ^{68}Ga chelators DOTA, NOTA and HBED-CC even when each of these ligands was labeled under its respective optimal conditions (heat and low pH for DOTA, low pH for NOTA and HBED) and longer incubation, while THP-Ac was used at room temperature and close to neutral pH after 1 – 5 minutes of incubation (60).

The positioning of the linker group at the center of the tripod ensures that the coordination properties are not greatly affected by attaching the chelator to biomolecules. Versions of THP with maleimide (**30**) (60) (for linkage to thiol groups), amine (63, 64) (for linkage to carboxylate groups, for example) and isothiocyanate linkers (**31**, **32**, Fig. 5)) (63, 64) have been synthesized and used to prepare labeled antibodies, and smaller proteins and peptides (64). *In vivo* studies with several of these new radiopharmaceuticals in animal cancer models have shown excellent *in vivo* stability and tumor imaging properties (e.g. **33**, Fig. 6) (60, 64).

The application of gallium chelators may not be restricted to PET imaging. The gamma-emitting isotope ^{67}Ga has been used for many years in the clinic, but its abundant and relatively high-energy Auger electron emissions, which have a range of track lengths commensurate with the dimensions of a cell (compared to the majority of Auger electron-emitters whose electrons have ranges in the order of nanometers) offer the possibility of radionuclide therapy of cancer, at least in theory. This has yet to be demonstrated successfully *in vivo* (68) but *in vitro* data indicate that intracellular ^{67}Ga is at least as toxic on a per-decay basis as ^{111}In (69), which has been clinically evaluated for radionuclide therapy (70). If this potential can be realized, the “theranostic” pair combining ^{68}Ga PET with ^{67}Ga therapy would have significant clinical application for both targeted detection and treatment of tumors.

3.3 Zirconium-89: “the new indium-111” – immunoPET and cell tracking

Although short half-life radionuclides are preferred where possible in order to keep radiation doses to patients as low as possible, in many applications the localization and clearance processes are slow, and long periods between injection of the tracer and imaging are required to develop adequate target-to-background ratio. In these instances, longer half-life tracers are needed. In single photon imaging this is conventionally achieved with ^{111}In, which can be attached to slow-localizing molecules like monoclonal antibodies (71) using bifunctional chelators, usually DTPA (72–74) (Fig. 1) and DOTA (Fig. 5) derivatives. With the increasing availability of PET, a longer half-life positron emitter has inevitably emerged as the PET analogue of ^{111}In: zirconium-89. The Zr^{4+} ion is not effectively chelated by conventional chelators such as DTPA, DOTA etc. that have found use with indium and other tricationic metals; indeed, very little work has been done to optimise ligand design for Zr^{4+}. Somewhat fortuitously, the siderophore desferrioxamine B (DFO, **25**, Fig. 5) has proved to be remarkably effective, despite being only hexadentate (whereas Zr^{4+} typically is eight-coordinate). PET with ^{89}Zr has now been used to follow the biodistribution and targeting of a number of antibodies in animal models and humans using the DFO method (75). Although evidence of significant instability of the zirconium-DFO complex *in vivo* is not conclusive even over several days, several groups are working to devise new ligand systems to optimize labeling efficiency and stability. The most popular approach is based on siderophore-like ligands but extended from hexadentate to octadentate (76). We have evaluated the THP ligands described above (**30**) for $^{89}Zr^{4+}$ chelation, and although *in vitro* their labeling properties and affinity constants are superior to those of DFO *in vitro*, the *in vivo* stability of the THP complex (attached to a monoclonal antibody via the maleimide linker) was markedly inferior to the DFO conjugates over a period of several days (77).

A second area of application of longer-lived radionuclides is that they can be incorporated into living cells to track their migration *in vivo* by imaging. This has been routinely used clinically for imaging the migration of leukocytes which have been isolated from the patients' peripheral blood, radiolabelled (conventionally with ^{111}In (78) or ^{99m}Tc (79–82)) and re-injected in order to locate hidden sites of infection and inflammation using a gamma camera. The most widely used cell labeling method utilizes lipophilic metastable six-coordinate complexes of $^{111}In^{3+}$ with three monobasic bidentate ligands, such as the tris(oxinate) (**34**, Fig. 7) and the tris(tropolonate) complexes, which diffuse non-specifically into cells by virtue of their lipophilicity, but dissociate inside cells in the presence of competing ligands. A PET analogue of this imaging method would offer the necessary improvements in sensitivity, quantification and resolution needed to address new challenges in cell tracking, such as clinical trials of cellular therapies and the development of methods to isolate specific subtypes of endogenous leukocytes (80, 83). ^{89}Zr has the potential to meet this need. Despite its preferred oxidation state of IV rather than III, zirconium shows parallel behavior to indium and can form eight-coordinate complexes with four such ligands. Oxine, tropolone and other monobasic bidentate ligands have been evaluated for cell labeling, and so far the oxinate complex (**35**, Fig. 7) has emerged as the lead candidate (84). The ^{89}Zr tetrakis(oxinate) complex is readily synthesized and labels cells efficiently and with prolonged stability, succeeding where other PET tracers evaluated for cell tracking (e.g. copper isotopes, see below) have failed. Not only does it have the advantage of PET imaging (compared to gamma imaging), but the cells also show more stable labeling (i.e. less loss of radioactivity over a period of days *in vivo*) and better cell survival than cells labeled with ^{111}In (85). A variety of human cell types and cultured cell lines have now been labeled by this method and it appears to be generally applicable as the first stable, robust method for cell labeling with a long half-life positron emitter. Many clinical applications in detection of inflammation, infection and early evaluation of cellular therapies are envisaged.

4 Copper: Exploiting Redox Chemistry

4.1 Copper isotopes and bioconjugates

Copper has several positron emitting radionuclides with a range of half-lives suited to different applications. The most generally useful is the cyclotron-produced isotope ^{64}Cu, with a half-life of 12.7 h. It has a complex decay profile, with three principal decay modes: positron (18%), electron capture (43%, accompanied by Auger electron emission) and beta emission (39%). All these offer potential for radionuclide therapy and hence ^{64}Cu has "theranostic" potential, although the therapeutic aspect has not been exploited clinically. The low energy of the positron (0.65 MeV) allows high-resolution PET imaging, and its relatively long half-life makes it useful for preclinical laboratory research as well as for clinical applications that require prolonged scanning (>24 h). For applications not requiring delayed imaging (e.g. small peptides, proteins and complexes), shorter half-life isotopes are preferred and ^{60}Cu (cyclotron produced, half life 20 min), ^{61}Cu (cyclotron-produced, half-life 3.3 h) and ^{62}Cu (half-life 9 min, produced from the ^{62}Zn/^{62}Cu generator) are suitable. The radiochemistry and application of copper isotopes has been reviewed many times, but still the most comprehensive review available (86), published in 1996, is now very much out of date and needs a thorough update.

Neither of the two preferred oxidation states, Cu(I) or Cu(II), offer great kinetic inertness. Cu(I), as a d^{10} ion, is particularly vulnerable to ligand exchange and has been very little used in radiopharmaceuticals, although preliminary work using Cu(I) bis(diphosphine) complexes has shown that the synthesis could be sufficiently rapid and efficient for use with the very short half-life isotope ^{62}Cu (87, 88). Diphosphine ligands **36** – **40** (Fig. 8) have been used to generate lipophilic cationic complexes Cu(diphosphine)$_2^+$, some of which served as substrates for the P-glycoprotein (MDR-1) and could therefore be used for PET imaging of multi-drug resistance in tumors (89). The diphosphine ligands could be derivatized as anhydride (**41**) and carboxylic acid (**42**) derivatives (Fig. 8) and thus serve as bifunctional chelators, providing sufficient biological stability to be useful for labeling biomolecules (88). Where labeling of biomolecules with long-term *in vivo* stability is necessary, Cu(II) is preferred and stability has to be enforced by polydentate macrocyclic amine and aminocarboxylate ligands. Even macrocycle-based ligands such as cyclam (**43**), TETA (**44**), DOTA (**22**, Fig. 5) and NOTA (**23**, Fig. 5) are perceived as inadequate to enforce the *in vivo* stability required for some applications, and cross-bridged macrocycles and bicyclic ligands such as and its cross-bridged forms of TETA and DOTA (e.g. **45**) have been introduced to overcome this problem (Fig. 8). Cross-bridged derivatives indeed offer improved *in vivo* stability, but at the expense of slower complex formation, requiring harsher labeling conditions (e.g. heat) that may be incompatible with some biomolecules. The sarcophagine-based ligands that are of key historical significance in the development of macrocyclic chemistry have been adapted by incorporation of linkers for use as copper bifunctional chelators for biomolecule labeling (**46**, Fig. 8), including “divalent” receptor-targeting molecules with peptides linked at both ends of the cage (**47**, Fig. 8) (90); they offer an appropriate balance of mild labeling conditions combined with excellent *in vivo* stability, and perform well in head-to-head *in vivo* comparison with other candidate copper chelators (91).

4.2 Bioreductive trapping – imaging blood flow and hypoxia

While other positron-emitting radiometals (e.g. ^{89}Zr, above) may be more suitable for labeling biomolecules where *in vivo* kinetic stability is required, copper has a unique attribute that other radiometals do not: a simple, controllable redox chemistry that can be manipulated and exploited for molecular imaging purposes. The intracellular reduction of Cu(II) to Cu(I) is a biologically feasible process that leads to instability of chelate complexes and is believed to represent a major pathway for undesirable metal-ligand dissociation in copper bioconjugates. For other purposes, however, bioreduction offers a versatile and useful mechanism of trapping radiocopper within cells. This possibility was first recognized in the cellular trapping mechanism of the blood flow tracer CuPTSM (**48**, Fig. 9) (92), a bis(thiosemicarbazone) (BTSC) complex labeled with ^{62}Cu or ^{64}Cu. Use of PET to quantitatively map blood flow requires a tracer that is trapped in cells efficiently and indiscriminately so that the uptake of tracer in a tissue is dependent only on its delivery via blood and not on other tissue or cell characteristics. Bioreduction provides this mechanism for CuPTSM (93), which is believed to be as follows: the complex is a small, planar, lipophilic molecule that is able to readily diffuse through cell membranes to reach the intracellular milieu, where it encounters cellular reducing agents (the identity of which is unknown or the subject of debate) and is reduced to a Cu(I) species. This species rapidly

dissociates, releasing the Cu(I) to become bound to intracellular macromolecules and thus trapped within the cell. In the case of CuPTSM the reduction and dissociation, and hence trapping, of copper is so rapid that it is almost independent of variations in cell metabolism between tissues and indeed is roughly proportional to blood flow.

A remarkable feature of the BTSC complexes is that their biological behavior can be exquisitely tuned by variation in alkylation at the diimine backbone and at the amino termini (Fig. 9). Indeed, these two sites offer a degree of independent control of reduction potential and lipophilicity, respectively. The sequential replacement of the two backbone hydrogens of the "parent" CuGTS with alkyl groups lowers the Cu(II)/Cu(I) reduction potential in steps of roughly 60 mV per alkyl group (as measured by cyclic voltammetry in DMSO solution) making the complexes progressively harder to reduce. Meanwhile, replacement of the hydrogens of the terminal amine groups by alkyl groups has relatively little effect on redox potential, but influences the lipophilicity and thereby cell permeability and pharmacokinetics (94–97). These features can even be varied and optimized by means of a combinatorial approach in which a mixture of several diketone and thiosemicarbazide components are reacted to create a library of BTSC ligands (98).

The structural, mechanistic and electronic structure features of CuBTSM complexes, especially the role of the backbone alkyl groups, underlying these structure activity relationships have been investigated in some detail. Cyclic voltammetry showed that backbone alkyl groups not only shift the Cu(II)/Cu(I) reduction potential by ca. 60 mV per alkyl group, but also make the reduction process more reversible (i.e. delay the acid-catalyzed dissociation) (99); while reduction of CuATSM (**50**, Fig. 9) was reversible in DMSO, it was rendered irreversible by addition of acetic acid. CuPTSM required less acid to make the reduction irreversible, while reduction of CuGTSM (**51**) was so sensitive to protons that reversible electrochemistry could only be observed in scrupulously dried DMSO. Density functional calculations showed that the effect of the backbone methyl groups in lowering the Cu(II)/Cu(I) redox potential could be predicted from theory (99), and variation in calculated structures and HOMO/LUMO energy levels induced by varying either backbone alkylation or replacing sulfur donor atoms with selenium, matched experimental results (X-ray crystal structures, electronic spectroscopy, EPR spectroscopy, cyclic voltammetry) very well (100). A series of X-ray crystal structures also demonstrated a subtle effect by which the presence of backbone alkyl groups was amplified to induce a significant shortening of the copper-sulfur bond lengths in the CuBTSC complexes (101). This shortening could be expected to increase electron donation by sulfur to copper. This too was predicted by the density functional calculations and may be an important contributor to the lower reduction potential.

The effect of backbone alkylation in making reduction harder and delaying dissociation post-reduction, combined with the ability of the reduced species to be re-oxidized to the Cu(II) BTSC complex by molecular oxygen, creates a potential mechanism for hypoxia-selective trapping of copper within the cell, and hence a means of PET imaging of hypoxic tissue – a valuable clinical tool because of the importance of hypoxia in many diseases, especially in relation to radiotherapy of cancer. This potential has indeed been realized with the prototype hypoxia imaging complex CuATSM, which is related to CuPTSM by

substitution of the hydrogen in the backbone by a methyl group, turning it from a blood flow imaging agent into a hypoxia imaging agent (102). The hypoxia selectivity of CuATSM has been experimentally confirmed both in cultured cells *in vitro* and in animal models. A rationale for the hypoxic selective trapping of copper with CuATSM, based on the physicochemical observations described above, is as follows (96, 100): the complex enters cells and is subject to intracellular bioreduction as described above. Because of the lower redox potential, reduction may be slower and the complex may thus have more time to diffuse out of the cell - unless the environment is hypoxic, where a more reducing environment increases the likelihood of tracer reduction and dissociation even in complexes with low redox potential because of their backbone alkylation. This mechanism relies only on the low redox potential to create selectivity. An additional level of selectivity may arise from the additional reversibility of the reduction process endowed by the backbone alkyl groups; once reduced, the reduced species dissociates more slowly, allowing time for the complex to be re-oxidized by molecular oxygen (it is known from chemical reactivity studies that the reduced species can be re-oxidized by O_2 (99)) whereupon it can diffuse back out of the cell and be cleared; hence dissociation and trapping only occurs if oxygen is limited.

^{60}CuATSM, ^{62}CuATSM and ^{64}CuATSM have all been evaluated in clinical trials in cancer patients, and shown some promise for predicting the outcome of radiotherapy (103–106). ^{64}CuATSM has also been shown to be more toxic to hypoxic cells than to normoxic cells, simply by virtue of the increased uptake in hypoxic cells (107). However, not all of the preclinical and clinical evaluations of hypoxia imaging have produced encouraging results, and the principle of hypoxia selectivity of CuATSM *in vivo* remains subject to some discussion (106, 108). Some studies indicate that CuATSM uptake is regulated primarily by hypoxia while others conclude that blood flow is the main determinant. It has also been suggested that the biodistribution of CuATSM may reflect the behavior of ionic copper rather than the intact CuATSM complex (108), although given the very different biodistribution of several different CuBTSC complexes (see above and below) this seems unlikely. An additional non-ideal feature of CuATSM, which it appears to share with most other current hypoxia tracers, is that it is only trapped in cells suffering the most extreme hypoxia – when the oxygen partial pressure in the medium is below 0.1 mm Hg (96) - whereas the partial pressure of most interest clinically (e.g. to predict tumor radiation sensitivity or impaired cardiac energetics) is much higher (ca. 20 mm Hg is the threshold below which cellular radiosensitivity begins to drop substantially). This extremely low threshold suggests that only a very small subset of cells in a hypoxic region of tumor will be hypoxic enough to trap the tracer, and consequently the uptake will be much lower than optimal leading to images with limited clinical usefulness (109).

Given the clear indication from *in vitro* studies that CuBTSC complexes with two alkyl groups in the diimine backbone are selectively trapped in hypoxic cells, efforts to overcome these non-ideal hypoxic targeting properties of CuATSM are warranted. Possible strategies are to investigate the mechanism of trapping to identify other potential features that may control tracer uptake, and to modify the pharmacokinetic properties of the system by varying tracer lipophilicity. As an approach towards both of these objectives we have adopted the Langendorff isolated perfused rat heart model, which offers the advantage of being an

efficient flow-through intact organ preparation (with consequent major advantages over cell culture systems) without the complexity and lack of control associated with *in vivo* models. It is of course also directly relevant to imaging hypoxia in the myocardium, which is of interest but currently underdeveloped as a diagnostic technique in cardiology (110). This system, indeed, was used to demonstrate the hypoxia selectivity of CuATSM for the first time (102). It offers almost complete experimental control and monitoring of the oxygenation, flow rate, energy consumption, and contractile performance characteristics, while allowing monitoring of radiotracer trapping or washout with sub-second temporal resolution. It allows several tracers to be evaluated rapidly in sequence under varied conditions, for example by switching the perfusion buffer from oxygenated to anoxic (or intermediate levels of oxygenation), and pharmacokinetics can be modeled (111). None of these are effectively achieved in cell suspension systems (112). Some examples of the tracer uptake profiles are shown in Fig. 10. The system has been used to investigate three questions:

- Can features of tissue and cellular metabolism other than simple oxygenation (such as intracellular pH or thiol levels) influence copper retention after administration of CuATSM?
- Can complexes be found with improved pharmacokinetics (faster clearance from normoxic tissue) and hypoxic selectivity (higher uptake in hypoxic cells and/or lower uptake in normoxic cells)?
- Can complexes be found that “switch on” cellular trapping at less extreme levels of hypoxia, more aligned with levels at which clinical symptoms and consequences occur?

The first was addressed by pharmacological manipulation to increase intracellular glutathione levels significantly above normal, and to decrease them significantly below normal, in hearts to which CuATSM was then administered under normoxic and anoxic conditions. Neither hypoxic nor normoxic uptake was affected by these changes (113). Similarly, inducing acidosis did not affect the hypoxia dependence of copper trapping, despite suggestions based on the acid-dependence of dissociation of the reduced CuATSM species that acidosis might promote trapping. Thus, it was conclusively shown than neither increases in cellular reduced glutathione, nor decreases in cellular pH, are required to induce selective trapping of CuATSM in hypoxic cells; so far, no metabolic features other than oxygen concentration have been shown to influence tracer uptake directly.

The second question addresses a problem with selectivity of CuATSM which can be seen by inspection of Fig. 10. Although copper uptake in hypoxic hearts is several-fold higher than in normoxic hearts, there remains some significant residual uptake in normoxic hearts of about 10%. This provides a possible hypothesis to explain observations in several (not all) *in vivo* tumor model studies that CuATSM uptake reflects blood flow/perfusion rather than hypoxia. On the assumption that, in tumors, the most hypoxic cancer cells are likely to be those most distant from capillaries, to reach many of the hypoxic cells CuATSM molecules must traverse layers of oxygenated cells. The residual normoxic trapping evidenced in Fig. 10 would mean that much of the tracer would never reach the distal hypoxic cells. In these circumstances CuATSM becomes a rather inefficient flow tracer instead of a hypoxia tracer.

This hypothesis suggests that a less lipophilic version of the tracer would be less likely to enter proximal normoxic cells *en route* to the distal hypoxic tumor cells, and also may be cleared from normoxic tissues more quickly by spending less time sequestered within membranes. A study examining the dependence of the tracer uptake profile in the heart on lipophilicity and reduction potential of the CuBTSC complexes showed that this reasoning has value in identifying improved hypoxia tracers: two alternative analogues with reduced lipophilicity (by removing methyl groups from the terminal amine position), CuATS (**52**) and CuCTS (**53**) (Fig. 9), showed reduced trapping and faster clearance from normoxic hearts, and increased trapping in hypoxic hearts (i.e. both improved pharmacokinetics and improved hypoxia selectivity; Fig. 10) (114). On the other hand CuATSE (**54**, Fig. 9) (115), which is hypoxia-selective (having two backbone alkyl groups) but more lipophilic than CuATSM (having terminal ethyl instead of methyl groups) has a hypoxia-selective profile but achieves selectivity much more slowly because of delayed clearance (Fig. 10). This further exemplifies the value of controlling lipophilicity to improve biodistribution in different organ systems and disease states, as previously demonstrated by the fact that CuATSM crosses the blood brain barrier while the less lipophilic CuATS does not (116). This study also confirmed that complexes with fewer than two alkyl groups in the diimine backbone (CuPTSM) show uptake that is almost independent of oxygenation. The two improved hypoxia selective tracers CuATS and CuCTS are now being evaluated *in vivo* as hypoxia imaging agents.

To address the third question, of identifying BTSC complexes potentially capable of targeting clinically relevant degrees of chronic cardiac ischemia, we performed a series of hypoxic buffer titrations in Langendorff hearts to identify the threshold at which contractile function and cardiac energetics became compromised, but long term cardiac survival would still have been likely. To date most studies had only evaluated tracer retention in totally hypoxic/ischaemic hearts, which while useful, are of limited pathophysiological relevance. Using ^{31}P NMR spectroscopy, we determined that at 30% buffer oxygen saturation, cardiac phosphocreatine levels were compromised, but crucially, ATP levels were maintained. Cardiac contractility was compromised, lactate levels were elevated but not maximal (representative of residual mitochondrial reserve), and HIF1α levels were elevated – all consistent with energetic profiles characterizing chronically diseased myocardium clinically. When we then evaluated our tracer candidates under these conditions, CuCTS uniquely began to be taken up as pO2 reached this 30% oxygen saturation threshold, significantly sooner than any of the other tracers that we examined, including CuATSM (117). Encouragingly, *in vivo* studies in rats showed that CuCTS is not significantly taken up in the normoxic, normally functioning heart (114). Thus, by this approach, a tracer has emerged that warrants *in vivo* evaluation as a cardiac hypoxia imaging agent specifically tuned to detect hypoxia at levels relevant to cardiac disease. Encouragingly, *in vivo* studies in rats showed that CuCTS is not significantly taken up in the normoxic, normally functioning heart (114). Thus, by this approach, a tracer has emerged that warrants *in vivo* evaluation as a cardiac hypoxia imaging agent specifically tuned to detect hypoxia at levels relevant to cardiac disease.

4.3 Cell tracking with copper

We have seen above that CuBTSC complexes can be tuned to give redox potentials and lipophilicities suited to imaging of blood flow and hypoxia. The bioreductive intracellular trapping mechanism of CuBTSC complexes lends itself to further applications. One, at least conceptually, is cell labeling for cell tracking with ^{64}Cu, similar to that described above for ^{89}Zr. The aim in cell labeling is to incorporate ^{64}Cu into cells non-specifically and as efficiently as possible, and ensure that it is retained within the cell for the required duration of the *in vivo* tracking (i.e. ideally at least two half-lives). The BTSC complexes offer a simple solution to this: by choosing ligands that will give efficient reduction and trapping regardless of oxygen levels, it should be possible to achieve labeling of any cell type. Several groups have used ^{64}CuPTSM (118–120), as it is the most well-known of the non-hypoxia-selective BTSC ligands; however, the data in Fig. 10 shows that its trapping is not completely independent of hypoxia, while the cyclic voltammetry results described earlier suggest that ^{64}CuGTSM might have even more efficient cell labeling properties. Labeling human cancer cell lines with ^{64}CuGTSM indeed proved to be more efficient and rapid compared to ^{64}CuPTSM and other ^{64}CuBSTC complexes, with around 80% of radioactivity taken up in cultured cells of different types within a few minutes (121). Unfortunately, irrespective of which ^{64}CuBTSC complex was used (CuPTSM, CuGTSM and others), the radioactivity quickly washed out of the cells, with only about 20% of the initially trapped activity remaining by 24 h. Switching to an alternative form of bioreducible lipophilic complex – copper(II) bis(dithiocarbamate) complexes – produced similar very high labeling efficiencies but a similar rate of efflux (121). Thus, while the efficiency of labeling varied substantially with different BTSC and dithiocarbamate ligands, the rate of efflux was unaffected by the complex used. This is consistent with the original hypothesis that the complex undergoes dissociation within the cell, and once this has occurred the fate of the copper is independent of the chelator. The copper is excreted from the cell by equilibrium or native copper trafficking systems. Several authors, although often describing ^{64}CuPTSM as a “successful” cell tracking PET agent, have reported similar experiences (118–120), and it must be concluded that relying on intracellular dissociation of copper complexes is inadequate for long term cell tracking experiments, despite having been successful for ^{111}In and ^{89}Zr (perhaps because indium and zirconium are “abiological” elements and have no specific biological cellular trafficking mechanisms). If radiocopper is to be used for cell tracking, alternative methods must be found.

4.4 Copper trafficking pathways in health and disease

The failure of ^{64}CuBTSC complexes as cell tracking labels is likely to be a result of the ^{64}Cu being subject to native cellular transport mechanisms for copper. This same feature offers an alternative application of copper isotopes: using PET to study disease-related changes in the transport and metabolism of copper. Several diseases are characterized (as cause or consequence) to altered copper metabolism, including Wilson’s disease, Menkes’ disease, Niemann-Pick disease, various dementias, and nutritional abnormalities. ^{64}Cu transport changes have also recently been observed in some tumor models (122). ^{64}Cu has barely been used for this purpose so far. ^{64}Cu can be administered via different routes (diet, intravenously, hepatic portal vein, etc.) and in different forms (ionic copper, albumin, ceruloplasmin, etc.) to elucidate transport pathways by which copper can reach cells. In

addition, the ability of ^{64}CuGTSM to deliver ^{64}Cu non-selectively to all cells could be used to bypass these delivery systems and allow the efflux of copper from different tissues in health and disease to be studied. We have recently demonstrated this approach in a mouse model of Alzheimer's disease. When ^{64}Cu acetate is administered intravenously to mice, delivery to brain is very low and focused in the ventricular regions of the brain (Fig. 11). However, when ^{64}CuGTSM is administered by the same route, much more is taken up in brain and the uptake is global; there is also high uptake in all other tissues with high blood flow, especially the myocardium (Fig. 11). Intriguingly, the initially trapped activity in most tissues (notably the heart and lungs) is rapidly cleared over a few hours, but clearance from the brain is very low indeed. In the Alzheimer's disease model, while uptake in brain was increased compared to normal controls, clearance from brain between 30 min and 24 h was accelerated fivefold (Fig. 11), although this was still much slower than from other tissues (123). This study provides an example of the potential for use of copper radionuclides to study abnormalities in copper metabolism related to disease. Many applications of this approach can be imagined.

5 Inorganic Elements as Binding Sites for ^{18}F-Fluoride

PET radiochemistry with fluorine-18 is traditionally regarded as the preserve of organic chemists. However, recently a novel inorganic approach to labeling biomolecules with ^{18}F has emerged in which a coordinatively unsaturated aluminum complex is used as a high-affinity binding site for fluoride. Bifunctional molecules containing other elements with a high affinity for fluorine, including silicon and boron, have also been used for biomolecule labeling (5). We have used this approach to develop an ^{18}F-labelled PET agent for imaging the activity of the human sodium/iodide symporter (hNIS), for diagnosis of thyroid disease and for imaging hNIS when used as a reporter gene. Thyroid cancer and abnormal thyroid function have been a mainstay activity in nuclear medicine for half a century, using gamma-emitting isotopes ^{131}I and ^{123}I in the form of iodide. Iodide is the natural substrate of hNIS, which pumps it into the cell driven by the concentration gradient of sodium ions across the cell membrane. ^{99m}Tc imaging of hNIS is also routinely used, as the pertechnetate ion is also an efficient hNIS substrate, although unlike iodine it is not metabolically trapped within the thyroid. The advantages of PET imaging of thyroid disease have been sought by use of the positron emitter ^{124}I, but the half-life of this isotope (4.2 days) is excessive and the positron yield is low, while unwanted gamma emissions are high; all these features contribute to excessive radiation dose to patients and inferior quality imaging. A tracer labeled with ^{18}F would be advantageous in all these respects, as well as being very readily available. The tetrafluoroborate ion is a substrate of hNIS, and we have developed an effective method of producing ^{18}F-labelled BF_4^- with a yield and specific activity sufficient for clinical PET imaging. Preclinical imaging in mice demonstrated excellent target to background ratios and excellent quality images, with greatly increased uptake in a thyroid tumor model. Specificity for hNIS as the mechanism of uptake was demonstrated by administering perchlorate, which is a competitive inhibitor/substrate of hNIS (Fig. 12) (124, 125). This new thyroid PET imaging agent is now undergoing clinical trials in patients with thyroid cancer and salivary gland cancer.

6 Multimodality Imaging and Nanoparticulate Contrast Agents

Much of the new chemistry described in this article has been driven by a shift in imaging technology towards PET during the last 20 years (which was in turn driven by the importance of the glucose tracer FDG, which has no gamma-emitting analogue). Currently another shift in technology is underway, in which different imaging modalities are combined so that they may complement each other to overcome limitations of the individual modalities. For example, PET and SPECT have exquisite sensitivity (that is, very small amounts of contrast agent – sub-picomolar concentrations *in vivo* – are required to produce images) and they provide truly "molecular" imaging; however, they suffer from poor resolution (ca. 1 cm in humans). Magnetic resonance imaging (MRI), on the other hand, offers much better anatomical resolution but its molecular imaging capability is restricted by the large amounts of contrast agent required (ca. milli/micromolar *in vivo*) because of its poor sensitivity. Optical imaging can be used at both the whole body (at least in small animals) and cell level, whereas radionuclide imaging cannot; but optical imaging is severely restricted in its clinical use by scatter and poor tissue penetration of visible light; combining the two can therefore provide cellular mechanistic information to help interpret whole body scanning. A new generation of scanners combining PET and MRI is now entering clinical use, and once again this new technology is driving new chemistry to produce combined modality contrast agents.

One approach to combined radionuclide and magnetic contrast agents is to incorporate radionuclides into magnetic nanoparticles (e.g. superparamagnetic iron oxide nanoparticles (SPION)) and other non-magnetic inorganic materials. Nanoparticles have potential in specific niche areas of imaging such as sentinel lymph node localization (126), imaging the reticuloendothelial system (liver, spleen, bone marrow), exploiting the enhanced permeability and retention (EPR) effect associated with the disorganized neovasculature of tumors, cell labeling (81) and imaging liposome-mediated drug and gene delivery (127). To produce a stable and versatile link between radionuclide and nanoparticle surface, we have adopted an approach of devising chemistry that links directly to the inorganic material rather than the conventional approach of embedding the particles in an organic or silica matrix. We have found that the bisphosphonate group, well-established as a means of targeting bone mineral metabolism with radionuclides (in part because of the high affinity of bisphosphonates for hydroxyapatite), forms very high affinity and kinetically stable links with the surface of SPIONs (much more stable than the conventionally used carboxylate groups). This has been exploited by means of the dipyridylamino- and dithiocarbamato-bisphosphonate conjugates described above (Fig. 3). The dpa-bisphosphonate was used to link the $^{99m}Tc(CO)_3^+$ core to iron oxide-based nanoparticles, creating a dual modality SPECT/MRI contrast agent (18). A clinical trial to evaluate the advantages of this combination in breast cancer surgery (including intraoperative use of a hand held magnetometer to help locate the sentinel node) is now underway, using presurgical SPECT and MRI to locate sentinel lymph nodes (using the high sensitivity of the SPECT component) and to elucidate their internal structure and detailed local anatomy (using the MRI component). The SPION-bisphosphonate interaction can also be used to modify the surface of the nanoparticles to control their clearance half-life in blood (by attaching

polyethylene glycol (PEG)) (17) and potentially to add molecular targeting capability. The dithiocarbamate-bisphosphonate conjugate, described above for synthesis of a ^{99m}Tc-divalent bisphosphonate complex for imaging calcification (Fig. 3), was used to produce a ^{64}Cu bis(dithiocarbamate) complex **55**, also with two pendant bisphosphonate groups, that afforded extremely stable binding of ^{64}Cu to the iron oxide surface (Fig. 13), allowing combined modality PET and MRI of lymph nodes *in vivo* (128).

A second approach to the design of nanoparticulate contrast agents is to identify materials for the fabrication of nanoparticles in which the material itself has a high affinity for the most useful radionuclides – notably ^{18}F-fluoride. Several inorganic nanoparticulate materials have been identified that bind fluoride with high affinity and stability, in some cases with extraordinary capacity and very simple labeling procedures (129). The leading candidates were hydroxyapatite and aluminum hydroxide. As well as providing readily-labeled particulates for PET imaging, these materials can be combined with SPIONs to afford the advantages of combined MRI and radionuclide imaging, by constructing core-shell nanoparticles with an iron oxide based material encapsulated in a biocompatible shell of aluminum hydroxide (23) or hydroxyapatite (130), both of which are biocompatible and endow the particles with high affinity for ^{18}F-fluoride. These shell materials also have a high affinity for bisphosphonate groups, so that the radiolabelled or PEG-linked bisphosphonate derivatives can also be used to radiolabel or modify their surfaces. Similarly, these materials can also be rendered fluorescent for optical imaging by attaching fluorophores covalently linked to bisphosphonate groups, yielding versatile trimodality contrast agents.

The complementarity of optical and radionuclide imaging is important to enable correlation of imaging at the whole body level with cellular imaging at the microscopic level. This is valuable in the basic study of cell trafficking processes such as cancer metastasis and the migration of immune cells and stem cells. Imaging tools to exploit this, both for basic biomedical studies in animal models and for application in clinical trials of cellular therapies, are sought after. In principle, cells can be engineered genetically to express a “reporter gene” which enables them to be detected by means of an imaging technique to show their location and function/survival in the body (131). The sodium/iodide symporter (hNIS) is an excellent example of such a gene because its expression in the host is restricted mainly to thyroid and stomach and it can be imaged with a wide range of simple radiotracers (iodine isotopes as described above, ^{99m}Tc-pertechnetate, and now ^{18}F-tetrafluoroborate, Fig. 12, center image). We have combined this with fluorescence imaging by creating a gene encoding a fusion protein combining both, and demonstrated the value of the combined modality imaging by detecting micrometastases with extremely high sensitivity in a cancer animal model, using ^{99m}Tc-pertechnetate SPECT (132) and ^{18}F-tetrafluoroborate PET.

7 Summary and Conclusion

The development of medical imaging is a highly multidisciplinary endeavor requiring the close cooperation of clinicians, physicists, engineers, biologists and chemists to identify capabilities, conceive challenges and solutions and apply them in the clinic. The chemistry described in this article illustrates how synergistic advances in these areas drive the technology and its applications forward, with each discipline producing innovations that in

turn drive innovations in the others. The main thread running through this article is the shift from single photon radionuclide imaging towards PET, and in turn the emerging shift from PET/CT towards PET/MRI and further, combination of these with optical imaging. At the same time, a renaissance of development of technetium chemistry may be anticipated by renewed confidence in the supply of ^{99m}Tc and the unmet need for simpler methods of radiolabelling compatible with biomolecular targeting. This would mimic progress in the current development of simple chemistry to exploit the ^{68}Ga generator, and methodology for cell tracking in the new era of cellular therapies. A slowing down of inorganic chemical innovation for application in medical imaging is not anticipated.

Acknowledgments

The authors are grateful to Dr Kavitha Sunassee and Mr Stephen Clarke for assistance with small animal imaging. This research was supported grants from the Alzheimer' Society, Alzheimer's Research UK, Leukaemia and Lymphoma Research, Cancer Research UK, EPSRC, by the Centre of Excellence in Medical Engineering funded by the Wellcome Trust and EPSRC under grant number WT088641/Z/09/Z, and the King's College London and UCL Comprehensive Cancer Imaging Centre funded by CRUK and EPSRC in association with the MRC and DoH (England), and by the National Institute for Health Research (NIHR) Biomedical Research Centre at Guy's and St Thomas' NHS Foundation Trust and King's College London. PET and SPECT scanning equipment was funded by an equipment grant from the Wellcome Trust. The views expressed are those of the author(s) and not necessarily those of the NHS, the NIHR or the Department of Health.

References

1. Blower PJ. Dalton Trans. 2015; 44:4819. [PubMed: 25406520]
2. Blower P. Dalton Trans. 2006:1705. [PubMed: 16568178]
3. Heilbron JL, S RW. Lawrence and his laboratory: a history of the Lawrence Berkeley Laboratory. University of California Press; Berkeley: 1989.
4. Miale AJ. J Florida Med Assoc. 1995; 82:749.
5. Smith GE, Sladen HL, Biagini SCG, Blower PJ. Dalton Trans. 2011; 40:6196. [PubMed: 21499604]
6. Dilworth JR, Parrott SJ. Chem Soc Rev. 1998; 27:43.
7. Bisunadan MM, Blower PJ, Clarke SEM, Singh J, Went MJ. Appl Radiat Isot. 1991; 42:167.
8. Blower PJ, Singh J, Clarke SEM. J Nucl Med. 1991; 32:845. [PubMed: 1850782]
9. Singh J, Powell AK, Clarke SEM, Blower PJ. J Chem Soc Chem Commun. 1991:1115.
10. Singh J, Reghebi K, Lazarus CR, Clarke SEM, Callahan AP, Knapp FF, Blower PJ. Nucl Med Commun. 1993; 14:197. [PubMed: 8384352]
11. Lam ASK, Puncher MRB, Blower PJ. Eur J Nucl Med. 1996; 23:1575. [PubMed: 8929310]
12. Lam ASK, Kettle AG, Odoherty MJ, Coakley AJ, Barrington SF, Blower PJ. Nucl Med Commun. 1997; 18:907. [PubMed: 9392790]
13. Blower PJ, Lam ASK, O'Doherty MJ, Kettle AG, Coakley AJ, Knapp FF. Eur J Nucl Med. 1998; 25:613. [PubMed: 9618576]
14. Blower PJ, Kettle AG, O'Doherty MJ, Coakley AJ, Knapp FF. Eur J Nucl Med. 2000; 27:1405.
15. Choudhry U, Greenland WEP, Goddard WA, Maclennan TAJ, Teat SJ, Blower PJ. Dalton Trans. 2003:311.
16. Bordoloi JK, Berry D, Khan IU, Sunassee K, de Rosales RTM, Shanahan C, Blower PJ. Dalton Trans. 2015; 44:4963. [PubMed: 25559039]
17. Sandiford L, Phinikaridou A, Protti A, Meszaros LK, Cui X, Yan Y, Frodsham G, Williamson PA, Gaddum N, Botnar RM, Blower PJ, et al. ACS Nano. 2013; 7:500. [PubMed: 23194247]
18. de Rosales RTM, Tavare R, Glaria A, Varma G, Protti A, Blower PJ. Bioconjugate Chem. 2011; 22:455.
19. de Rosales RTM, Finucane C, Foster J, Mather SJ, Blower PJ. Bioconjugate Chem. 2010; 21:811.
20. de Rosales RTM, Finucane C, Mather SJ, Blower PJ. Chem Commun. 2009:4847.

21. Kluba CA, Mindt TL. Molecules. 2013; 18:3206. [PubMed: 23481882]
22. Bartholoma M, Valliant J, Maresca KP, Babich J, Zubieta J. Chem Commun. 2009:493.
23. Cui X, Belo S, Krueger D, Yan Y, de Rosales RTM, Jauregui-Osoro M, Ye H, Su S, Mathe D, Kovacs N, Horvath I, et al. Biomaterials. 2014; 35:5840. [PubMed: 24768194]
24. Prakash S, Went MJ, Blower PJ. Nucl Med Biol. 1996; 23:543. [PubMed: 8832713]
25. Abiraj K, Mansi R, Tamma ML, Forrer F, Cescato R, Reubi JC, Akyel KG, Maecke HR. Chem Eur J. 2010; 16:2115. [PubMed: 20066690]
26. Glaser M, Howard MJ, Howland K, Powell AK, Rae MT, Wocadlo S, Williamson RA, Blower PJ. J Chem Soc Dalton Trans. 1998:3087.
27. Prakash SD, Blower PJ. The chemistry of rhenium in nuclear medicinePerspectives on Bioinorganic Chemistry. Hay R, Dilworth JR, Nolan KB, editorsVol. 4. JAI Press; Connecticut: 1999.
28. Ohta H, Yamamoto K, Endo K, Mori T, Hamanaka D, Shimazu A, Ikekubo K, Makimoto K, Iida Y, Konishi J, Morita R, et al. J Nucl Med. 1984; 25:323. [PubMed: 6321700]
29. Choudhry U, PJ B. Nucl Med Commun. 2006; 27:294.
30. Zhang JB, Yu Q, Huo JF, Pang Y, Yang S, He YN, Tang TT, Yang CC, Wang XB. J Radioanal Nucl Chem. 2010; 283:481.
31. Berry DJ, de Rosales RTM, Charoenphun P, Blower PJ. Mini-Rev Med Chem. 2012; 12:1174. [PubMed: 22931590]
32. Pasqualini R, Duatti A. J Chem Soc Chem Commun. 1992:1354.
33. Dijkgraaf I, Yim CB, Franssen GM, Schuit RC, Luurtsema G, Liu SA, Oyen WJG, Boerman OC. Eur J Nucl Med Mol Imaging. 2011; 38:128. [PubMed: 20857099]
34. Meszaros LK, Dose A, Biagini SCG, Blower PJ. Inorg Chim Acta. 2010; 363:1059.
35. King RC, Surfraz MB-U, Biagini SCG, Blower PJ, Mather SJ. Dalton Trans. 2007:4998. [PubMed: 17992285]
36. King R, Surfraz MB-U, Finucane C, Biagini SCG, Blower PJ, Mather SJ. J Nucl Med. 2009; 50:591. [PubMed: 19289435]
37. Surfraz MB-U, King R, Mather SJ, Biagini S, Blower PJ. J Inorg Biochem. 2009; 103:971. [PubMed: 19447500]
38. Meszaros LK, Dose A, Biagini SCG, Blower PJ. Dalton Trans. 2011; 40:6260. [PubMed: 21350776]
39. Greenland WEP, Howland K, Hardy J, Fogelman I, Blower PJ. J Med Chem. 2003; 46:1751. [PubMed: 12699393]
40. Surfraz MB-U, King R, Mather SJ, Biagini SCG, Blower PJ. J Med Chem. 2007; 50:1418. [PubMed: 17315986]
41. Surfraz MB-U, King R, Mather SJ, Biagini SCG, Blower PJ. Tetrahedron. 2010; 66:2037.
42. Surfraz MB-U, Biagini SCG, Blower PJ. Dalton Trans. 2008:2920. [PubMed: 18493625]
43. Guhlke S, Schaffland A, Zamora PO, Sartor J, Diekmann D, Bender H, Knapp FF, Biersack HJ. Nucl Med Biol. 1998; 25:621. [PubMed: 9804043]
44. Heinrich TK, Kraus W, Pietzsch HJ, Smuda C, Spies H. Inorg Chem. 2005; 44:9930. [PubMed: 16363864]
45. Waibel R, Alberto R, Willuda J, Finnern R, Schibli R, Stichelberger A, Egli A, Abram U, Mach JP, Pluckthun A, Schubiger PA. Nature Biotech. 1999; 17:897.
46. Kampmeier F, Williams JD, Maher J, Mullen GE, Blower PJ. Eur J Nucl Med Mol Imaging Res. 2014; 4:13.
47. Tavare R, De Rosales RTM, Blower PJ, Mullen GED. Bioconjugate Chem. 2009; 20:2071.
48. Tavare R, Williams J, Howland K, Blower PJ, Mullen GED. J Inorg Biochem. 2012; 114:24. [PubMed: 22687562]
49. Badar A, Williams J, de Rosales RT, Tavare R, Kampmeier F, Blower PJ, Mullen GE. Eur J Nucl Med Mol Imaging Res. 2014; 4:14.
50. Biechlin ML, d'Hardemare AD, Fraysse M, Gilly FN, Bonmartin A. J Labelled Comp Radiopharm. 2005; 48:873.

51. Williams JD, Cooper M, Kampmeier F, Tavare R, Mullen GE, Blower P. Eur J Nucl Med Mol Imaging. 2012; 39:S216.
52. Williams JD. PhD thesis: Site-specific radiolabelling of biomolecules with $[^{99m}Tc(CO)_3]^+$ and $[^{188}Re(CO)_3]^+$ complexes. King's College London; 2014.
53. Greenland WEP, Blower PJ. Bioconjugate Chem. 2005; 16:939.
54. Knapp FFR, Mirzadeh S, Beets AL, O'Doherty M, Blower PJ, Verdera ES, Gaudiano JS, Kropp J, Guhlke J, Palmedo H, Biersack HJ. Appl Radiat Isot. 1998; 49:309. [PubMed: 9519440]
55. Torres Martin de Rosales R, Blower PJ. The role of ^{99m}Tc in the development of rhenium radiopharmaceuticalsTechnetium radiopharmaceuticals: status and prospective. Duatti A, editorIAEA; Vienna: 2008. Technetium radiopharmaceuticals: status and prospective
56. Van Noorden R. Nature. 2013; 504:202. [PubMed: 24336269]
57. Blower PJ. Nucl Med Commun. 1993; 14:995. [PubMed: 8290173]
58. Rosch F. Appl Radiat Isot. 2013; 76:24. [PubMed: 23245638]
59. Price EW, Orvig C. Chem Soc Rev. 2014; 43:260. [PubMed: 24173525]
60. Berry DJ, Ma Y, Ballinger JR, Tavare R, Koers A, Sunassee K, Zhou T, Nawaz S, Mullen GED, Hider RC, Blower PJ. Chem Commun. 2011; 47:7068.
61. Liu ZD, Hider RC. Coord Chem Rev. 2002; 232:151.
62. Berry D. PhD thesis: Chelators for Gallium-68 Radiopharmaceuticals. King's College London; 2011.
63. Imberti C, Ma MT, Blower PJ. J Nucl Med. 2015; 56(supp 2) abstract 32.
64. Ma MT, Cullinane C, Roselt P, Imberti C, Hicks RJ, Blower PJ. J Nucl Med. 2015; 56(supp 2) abstract 45.
65. Imberti C, Nawaz S, Cooper MS, Young JD, Ma MT, Berry DJ, Patterson BM, Mullen GED, Ballinger JR, Blower PJ. J Nucl Med. 2015; 56(supp 2) abstract 33.
66. Blower PJ, Cooper MS, Nawaz S, O'Neill A, Koers A, Sunassee K, Berry DJ, Mullen GED, Ballinger JR. Eur J Nucl Med Mol Imaging. 2012; 39:S262.
67. Young JD, Cooper MS, Paterson BM, Ma MT, Ballinger JR, Nawaz S, Berry DJ, Hider RC, Mullen GED, Blower PJ. J Nucl Med. 2015; 56(supp 2) abstract 95.
68. Jonkhoff AR, Plaizier M, Ossenkoppele GJ, Teule GJJ, Huijgens PC. Br J Cancer. 1995; 72:1541. [PubMed: 8519674]
69. Othman MF, Terry SYA, Blower PJ. J Nucl Med. 2015; 56(supp 2) abstract 61.
70. Weeks AJ, Blower PJ, Lloyd DR. Nucl Med Biol. 2013; 40:73. [PubMed: 23062949]
71. Karagiannis P, Gilbert AE, Josephs DH, Ali N, Dodev T, Saul L, Correa I, Roberts L, Beddowes E, Koers A, Hobbs C, et al. J Clin Invest. 2013; 123:1457. [PubMed: 23454746]
72. Giersing BK, Rae MT, CarballidoBrea M, Williamson RA, Blower PJ. Bioconjugate Chem. 2001; 12:964.
73. Kulasegaram R, Giersing B, Page CJ, Blower PJ, Williamson RA, Peters BS, O'Doherty MJ. Eur J Nucl Med. 2001; 28:756.
74. Jolley C, Burnet FR, Blower PJ. Appl Radiat Isot. 1996; 47:623. [PubMed: 8759156]
75. Vugts DJ, Visser GWM, van Dongen G. Curr Topics Med Chem. 2013; 13:446.
76. Patra M, Bauman A, Mari C, Fischer CA, Blacque O, Haussinger D, Gasser G, Mindt TL. Chem Commun. 2014; 50:11523.
77. Ma MT, Meszaros LK, Paterson BM, Berry DJ, Cooper MS, Ma Y, Hiderd RC, Blower PJ. Dalton Trans. 2015; 44:4884. [PubMed: 25351250]
78. Puncher MRB, Blower PJ. J Nucl Med. 1995; 36:499. [PubMed: 7884517]
79. Puncher MRB, Blower PJ. Eur J Nucl Med. 1994; 21:1175. [PubMed: 7859768]
80. Lukawska JJ, Livieratos L, Sawyer BM, Lee T, O'Doherty M, Blower PJ, Kofi M, Ballinger JR, Corrigan CJ, Gnanasegaran G, Sharif-Paghaleh E, et al. J Allergy Clin Immunol. 2014; 133:233. [PubMed: 23953710]
81. McClelland CM, Onuegbulem E, Carter NJ, Leahy M, O'Doherty MJ, Pooley FD, O'Doherty T, Newsam RJ, Ensing GJ, Blower PJ. Nucl Med Commun. 2003; 24:191. [PubMed: 12548044]
82. Puncher MRB, Blower PJ. Eur J Nucl Med. 1995; 22:101. [PubMed: 7758495]

83. Lukawska JJ, Livieratos L, Sawyer BM, Lee T, O'Doherty MJ, Blower PJ, Kofic M, Ballinger JR, Corrigan CJ, Gnanasegeran G, Sharif-Paghaleh E, et al. EBioMedicine. 2014; 1:173. EBioMedicine. [PubMed: 26137523]
84. Ferris TJ, Charoenphun P, Meszaros LK, Mullen GED, Blower PJ, Went MJ. Dalton Trans. 2014; 43:14851. [PubMed: 25164373]
85. Charoenphun P, Meszaros LK, Chuamsaamarkkee K, Sharif-Paghaleh E, Ballinger JR, Ferris TJ, Went MJ, Mullen GED, Blower PJ. Eur J Nucl Med Mol Imaging. 2015; 42:278. [PubMed: 25359636]
86. Blower PJ, Lewis JS, Zweit J. Nucl Med Biol. 1996; 23:957. [PubMed: 9004284]
87. Lewis JS, Zweit J, Dearling JLJ, Rooney BC, Blower PJ. Chem Commun. 1996:1093.
88. Lewis JS, Heath SL, Powell AK, Zweit J, Blower PJ. J Chem Soc Dalton Trans. 1997:855.
89. Lewis JS, Dearling JLJ, Sosabowski JK, Zweit J, Carnochan P, Kelland LR, Coley HM, Blower PJ. Eur J Nucl Med. 2000; 27:638. [PubMed: 10901449]
90. Ma MT, Cooper MS, Paul RL, Shaw KP, Karas JA, Scanlon D, White JM, Blower PJ, Donnelly PS. Inorg Chem. 2011; 50:6701. [PubMed: 21667932]
91. Cooper MS, Ma MT, Sunassee K, Shaw KP, Williams JD, Paul RL, Donnelly PS, Blower PJ. Bioconjugate Chem. 2012; 23:1029.
92. Green MA, Klippenstein DL, Tennison JR. J Nucl Med. 1988; 29:1549. [PubMed: 3261785]
93. Shibuya K, Fujibayashi Y, Yoshimi E, Sasai K, Hiraoka M, Welch MJ. Annals Nucl Med. 1999; 13:287.
94. Dearling JLJ, Lewis JS, McCarthy DW, Welch MJ, Blower PJ. Chem Commun. 1998:2531.
95. Dearling JLJ, Lewis JS, Mullen GED, Rae MT, Zweit J, Blower PJ. Eur J Nucl Med. 1998; 25:788. [PubMed: 9662602]
96. Dearling JLJ, Lewis JS, Muller GED, Welch MJ, Blower PJ. J Biol Inorg Chem. 2002; 7:249. [PubMed: 11935349]
97. Blower PJ, Dilworth JR, Maurer RI, Mullen GD, Reynolds CA, Zheng YF. J Inorg Biochem. 2001; 85:15. [PubMed: 11377691]
98. Blower PJ, Went MJ, Martin KE, Smith GE. J Labelled Comp Radiopharm. 2007; 50:354.
99. Maurer RI, Blower PJ, Dilworth JR, Reynolds CA, Zheng YF, Mullen GED. J Med Chem. 2002; 45:1420. [PubMed: 11906283]
100. Castle TC, Maurer RI, Sowrey FE, Went MJ, Reynolds CA, McInnes EJL, Blower PJ. J Am Chem Soc. 2003; 125:10040. [PubMed: 12914467]
101. Blower PJ, Castle TC, Cowley AR, Dilworth JR, Donnelly PS, Labisbal E, Sowrey FE, Teat SJ, Went MJ. Dalton Trans. 2003:4416.
102. Fujibayashi Y, Taniuchi H, Yonekura Y, Ohtani H, Konishi J, Yokoyama A. J Nucl Med. 1997; 38:1155. [PubMed: 9225812]
103. Chia K, Fleming IN, Blower PJ. Nucl Med Commun. 2012; 33:217. [PubMed: 22146595]
104. Fleming IN, Manavaki R, Blower PJ, West C, Williams KJ, Harris AL, Domarkas J, Lord S, Baldry C, Gilbert FJ. Br J Cancer. 2015; 112:238. [PubMed: 25514380]
105. Yip C, Blower PJ, Goh V, Landau DB, Cook GJR. Eur J Nucl Med Mol Imaging. 2015; 42:956. [PubMed: 25701238]
106. Lapi SE, Lewis JS, Dehdashti F. Sem Nucl Med. 2015; 45:177.
107. Weeks AJ, Paul RL, Marsden PK, Blower PJ, Lloyd DR. Eur J Nucl Med Mol Imaging. 2010; 37:330. [PubMed: 19915836]
108. Hueting R, Kersemans V, Cornelissen B, Tredwell M, Hussien K, Christlieb M, Gee AD, Passchier J, Smart SC, Dilworth JR, Gouverneur V, et al. J Nucl Med. 2014; 55:128. [PubMed: 24337603]
109. Chia K, Weeks AJ, Paul RL, Cleij M, Blower PJ. Nucl Med Biol. 2010; 37:725.
110. Handley MG, Medina RA, Nagel E, Blower PJ, Southworth R. J Mol Cell Cardiol. 2011; 51:640. [PubMed: 21781973]
111. Mariotti E, Veronese M, Dunn JT, Medina RA, Blower PJ, Southworth R, Eykyn TR. Eur J Nucl Med Mol Imaging Res. 2013; 3:74.

112. Handley MG, Medina RA, Paul RL, Blower PJ, Southworth R. Nucl Med Commun. 2013; 34:1015. [PubMed: 23872986]
113. Shaughnessy F, Mariotti E, Shaw KP, Eykyn TR, Blower PJ, Siow R, Southworth R. Eur J Nucl Med Mol Imaging Res. 2014; 4:40.
114. Handley MG, Medina RA, Mariotti E, Kenny GD, Shaw KP, Yan R, Eykyn TR, Blower PJ, Southworth R. J Nucl Med. 2014; 55:488. [PubMed: 24421288]
115. McQuade P, Martin KE, Castle TC, Went MJ, Blower PJ, Welch MJ, Lewis JS. Nucl Med Biol. 2005; 32:147. [PubMed: 15721760]
116. Dearling JLJ, Mullen GED, Lewis JS, Welch MJ, Blower PJ. J Labelled Comp Radiopharm. 1999; 42:S276.
117. Medina RA, Mariotti E, Pavlovic D, Shaw KP, Eykyn TR, Blower PJ, Southworth R. J Nucl Med. 2015; 56:921. [PubMed: 25883129]
118. Huang J, Lee CCI, Sutcliffe JL, Cherry SR, Tarantal AF. Mol Imaging. 2008; 7:1. [PubMed: 18384718]
119. Park JJ, Lee TS, Son JJ, Chun KS, Song IH, Park YS, Kim KI, Lee YJ, Kang JH. Cancer Biother Radiopharm. 2012; 27:719. [PubMed: 23009582]
120. Adonai N, Nguyen KN, Walsh J, Iyer M, Toyokuni T, Phelps ME, McCarthy T, McCarthy DW, Gambhir SS. Proc Nat Acad Sci USA. 2002; 99:3030. [PubMed: 11867752]
121. Charoenphun P, Paul R, Weeks A, Berry D, Shaw K, Mullen G, Ballinger J, Blower PJ. Eur J Nucl Med Mol Imaging. 2011; 38:S294.
122. Hueting R. J Labelled Comp Radiopharm. 2014; 57:231. [PubMed: 24634197]
123. Torres JB, Andreozzi E, Gee A, Blower PJ. Eur J Nucl Med Mol Imaging. 2014; 41:S383.
124. Jauregui-Osoro M, Sunassee K, Weeks AJ, Berry DJ, Paul RL, Cleij M, Banga JP, O'Doherty MJ, Marsden PK, Clarke SEM, Ballinger JR, et al. Eur J Nucl Med Mol Imaging. 2010; 37:2108. [PubMed: 20577737]
125. Weeks AJ, Jauregui-Osoro M, Cleij M, Blower JE, Ballinger JR, Blower PJ. Nuc Med Commun. 2011; 32:98.
126. Brown K, Badar A, Sunassee K, Fernandes MA, Shariff H, Jurcevic S, Blower PJ, Sacks SH, Mullen GED, Wong W. Am J Transplantation. 2011; 11:225.
127. Mitchell N, Kalber TL, Cooper MS, Sunassee K, Chalker SL, Shaw KP, Ordidge KL, Badar A, Janes SM, Blower PJ, Lythgoe MF, et al. Biomaterials. 2013; 34:1179. [PubMed: 23131536]
128. de Rosales RTM, Tavare R, Paul RL, Jauregui-Osoro M, Protti A, Glaria A, Varma G, Szanda I, Blower PJ. Angew Chem Int Ed. 2011; 50:5509.
129. Jauregui-Osoro M, Williamson PA, Glaria A, Sunassee K, Charoenphun P, Green MA, Mullen GED, Blower PJ. Dalton Trans. 2011; 40:6226. [PubMed: 21394352]
130. Cui X, Green MA, Blower PJ, Zhou D, Yan Y, Zhang W, Djanashvili K, Mathe D, Veres DS, Szigeti K. Chem Commun. 2015; 51:9332.
131. Sharif-Paghaleh E, Sunassee K, Tavare R, Ratnasothy K, Koers A, Ali N, Alhabbab R, Blower PJ, Lechler RI, Smyth LA, Mullen GE, et al. PLOS One. 2011; 6:e25857. [PubMed: 22043296]
132. Fruhwirth GO, Diocou S, Blower PJ, Ng T, Mullen GED. J Nucl Med. 2014; 55:686. [PubMed: 24604910]

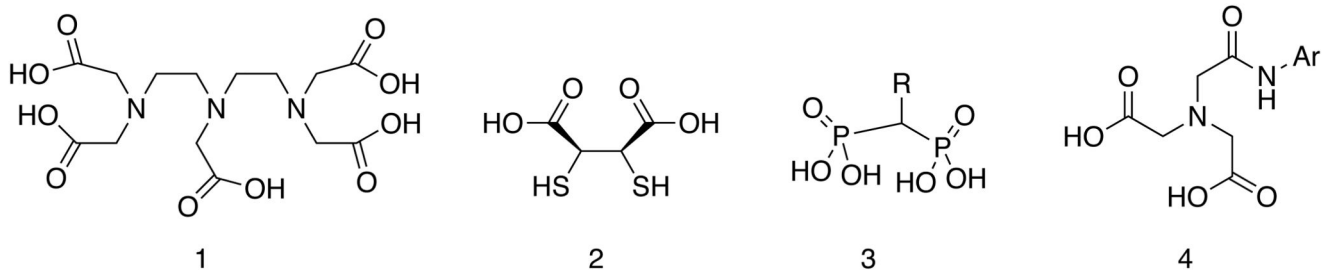

Figure 1.
Ligands used in first-generation ^{99m}Tc radiopharmaceuticals. The structures of the technetium complexes are not shown because in many cases they remain unknown.

Europe PMC Funders Author Manuscripts

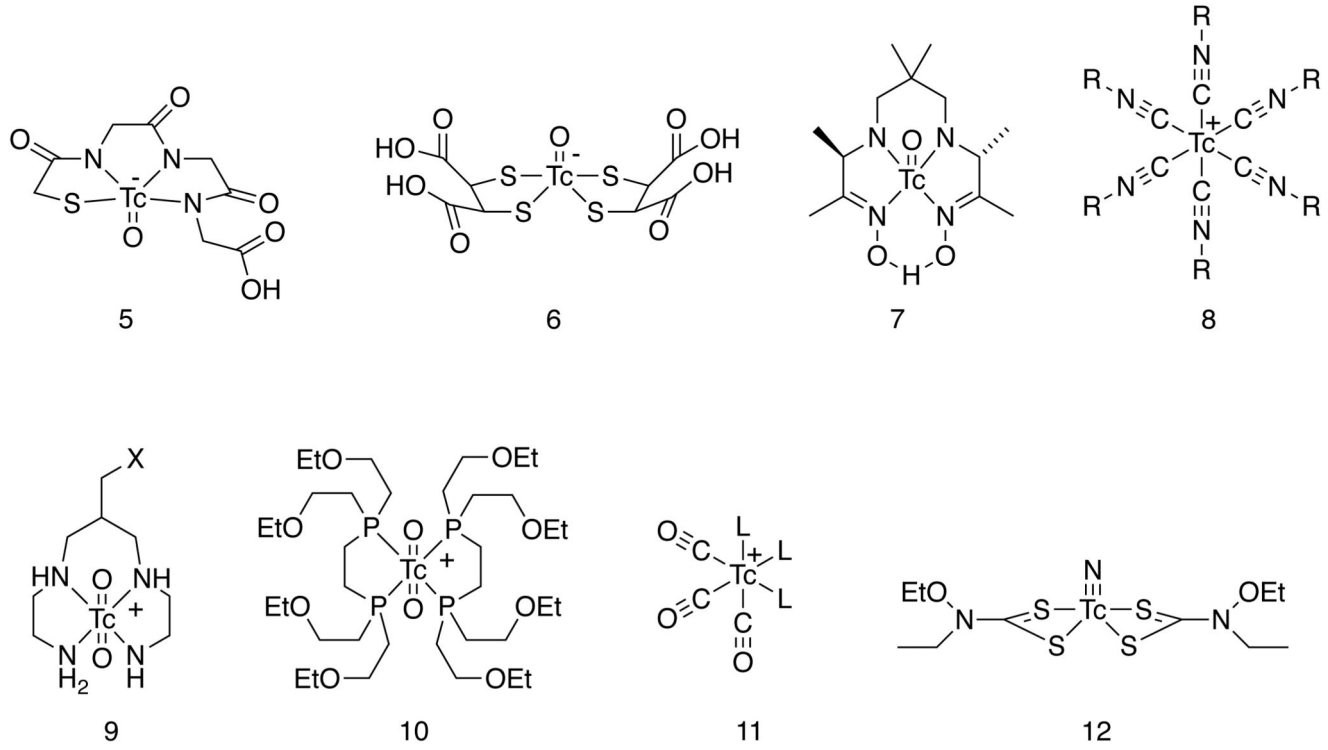

Figure 2.

Established “core complexes” of technetium with well-defined structure and high stability, used in current approaches to the design of ^{99m}Tc radiopharmaceuticals. X represents a linker group for bioconjugation.

Europe PMC Funders Author Manuscripts

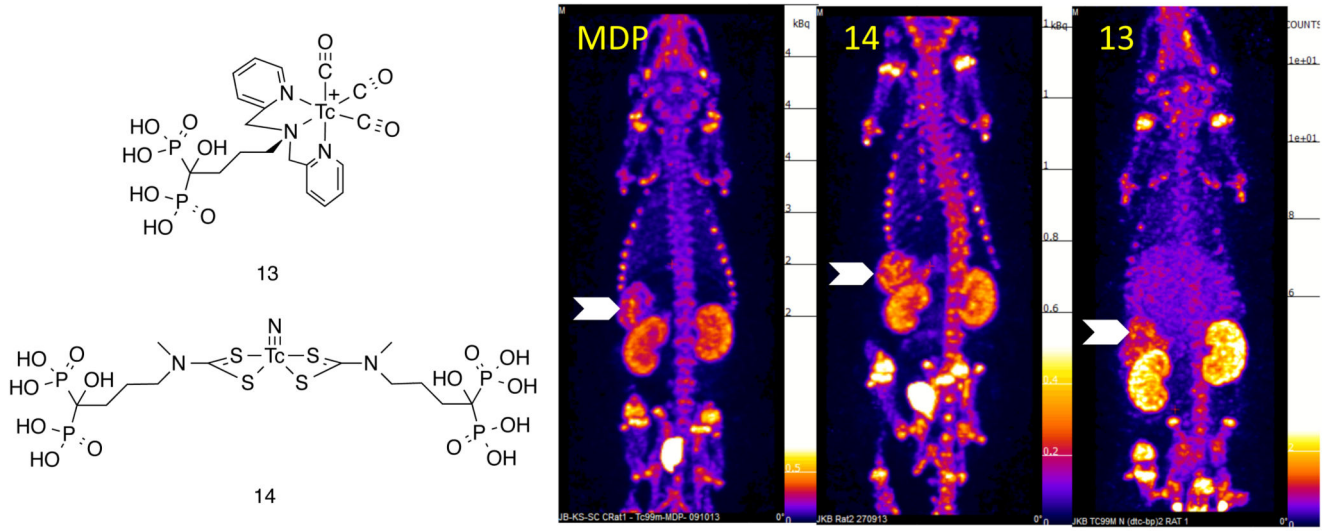

Figure 3.

Left: Bifunctional complexes of ^{99m}Tc linked to bisphosphonate groups. Right: SPECT images showing the biodistribution of (left to right respectively) conventional ^{99m}Tc bisphosphonate (**3**) complex of unknown structure, and bifunctional complexes **14** and **13**, in mice with systemic arterial and soft tissue calcification. As well as skeletal uptake typical of bisphosphonate complexes, strong uptake is seen in the calcified mesenteric arteries (arrows) and other soft tissues.

Europe PMC Funders Author Manuscripts

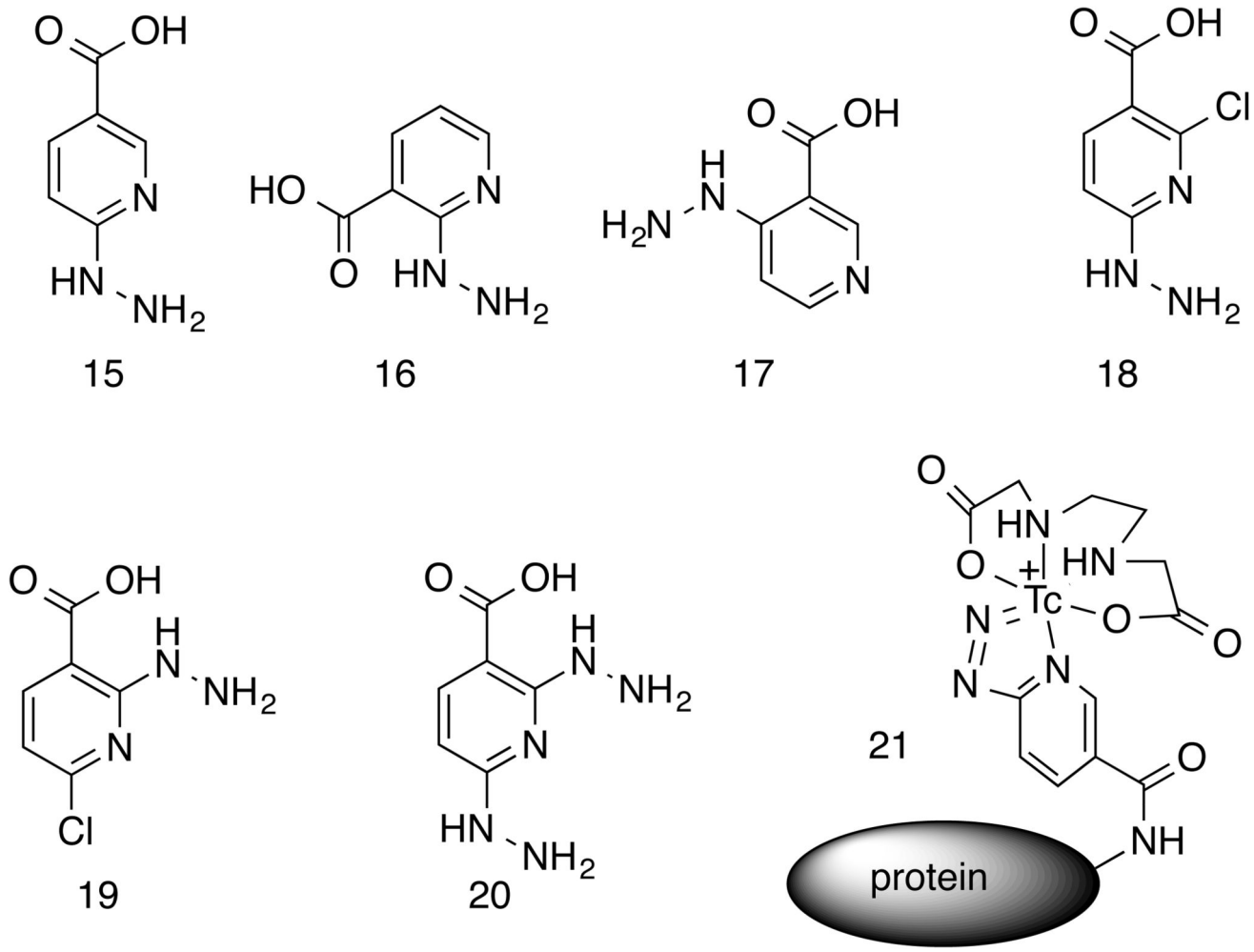

Figure 4.

Hydrazinonicotinamide (hynic) derivatives for synthesis of bioconjugates of ^{99m}Tc. Structure **15** is the prototypical hynic, while **16** – **20** are variants synthesized for comparison. Structure **21** represents a likely (bidentate) coordination mode of the hynic, with the coordination sphere completed by ethylenediaminediacetic acid (edda).

Europe PMC Funders Author Manuscripts

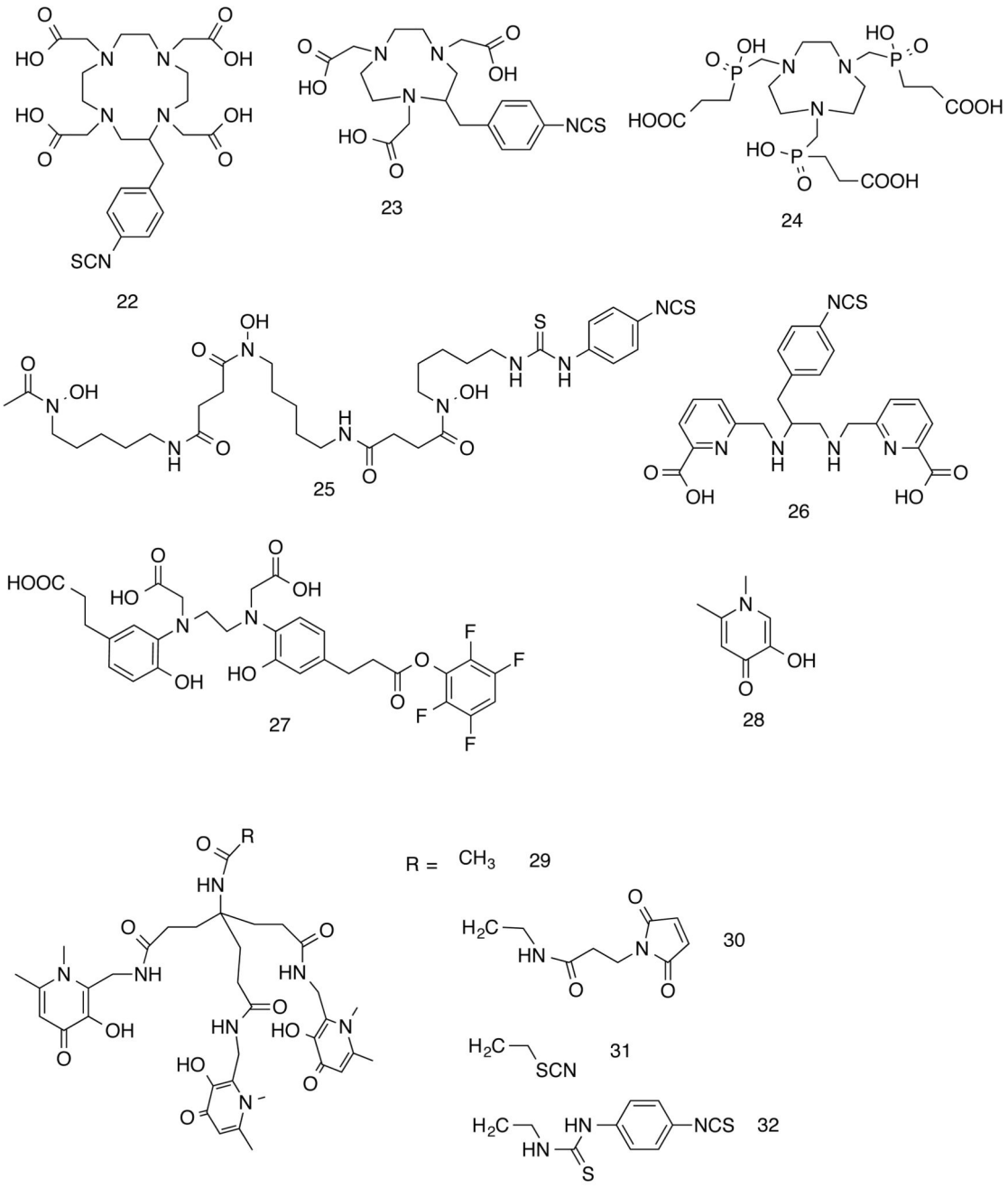

Figure 5.

Chelators and building blocks established and under development for incorporation of ^{68}Ga into radiopharmaceuticals. Commonly used names for the chelating groups are as follows: DOTA (**22**), NOTA (**23**), TRAP (**24**), desferrioxamine (DFO, **25**) DEDPA (**26**), HBED-CC (**27**), Deferiprone (**28**), THP (**29**-**32**).

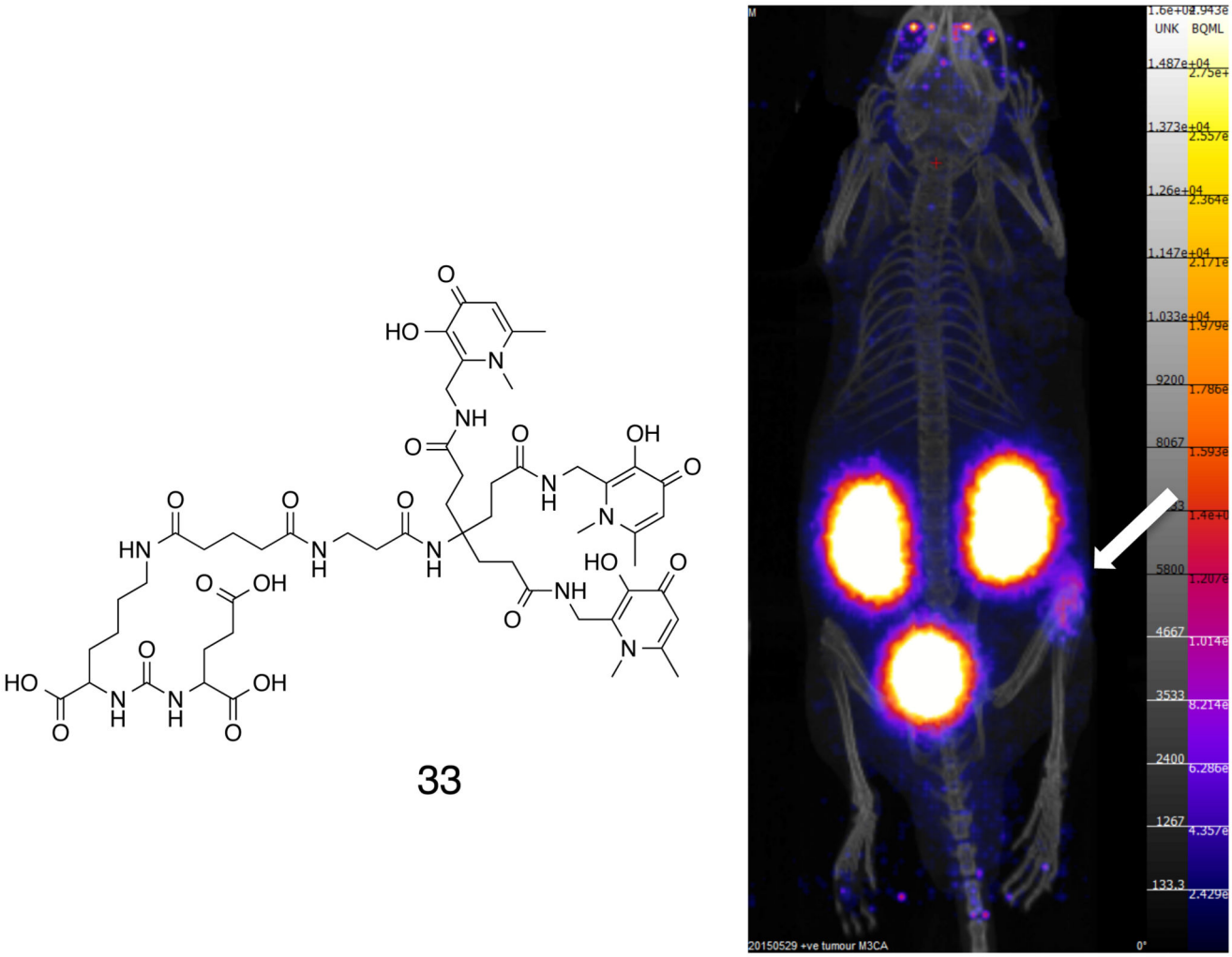

Figure 6.

Structure of a conjugate of a THP chelator with a ligand that binds to the prostate-specific membrane antigen (PSMA), and nanoPET/CT images showing specific tumor targeting (arrow) in a mouse model of PSMA-expressing prostate cancer.

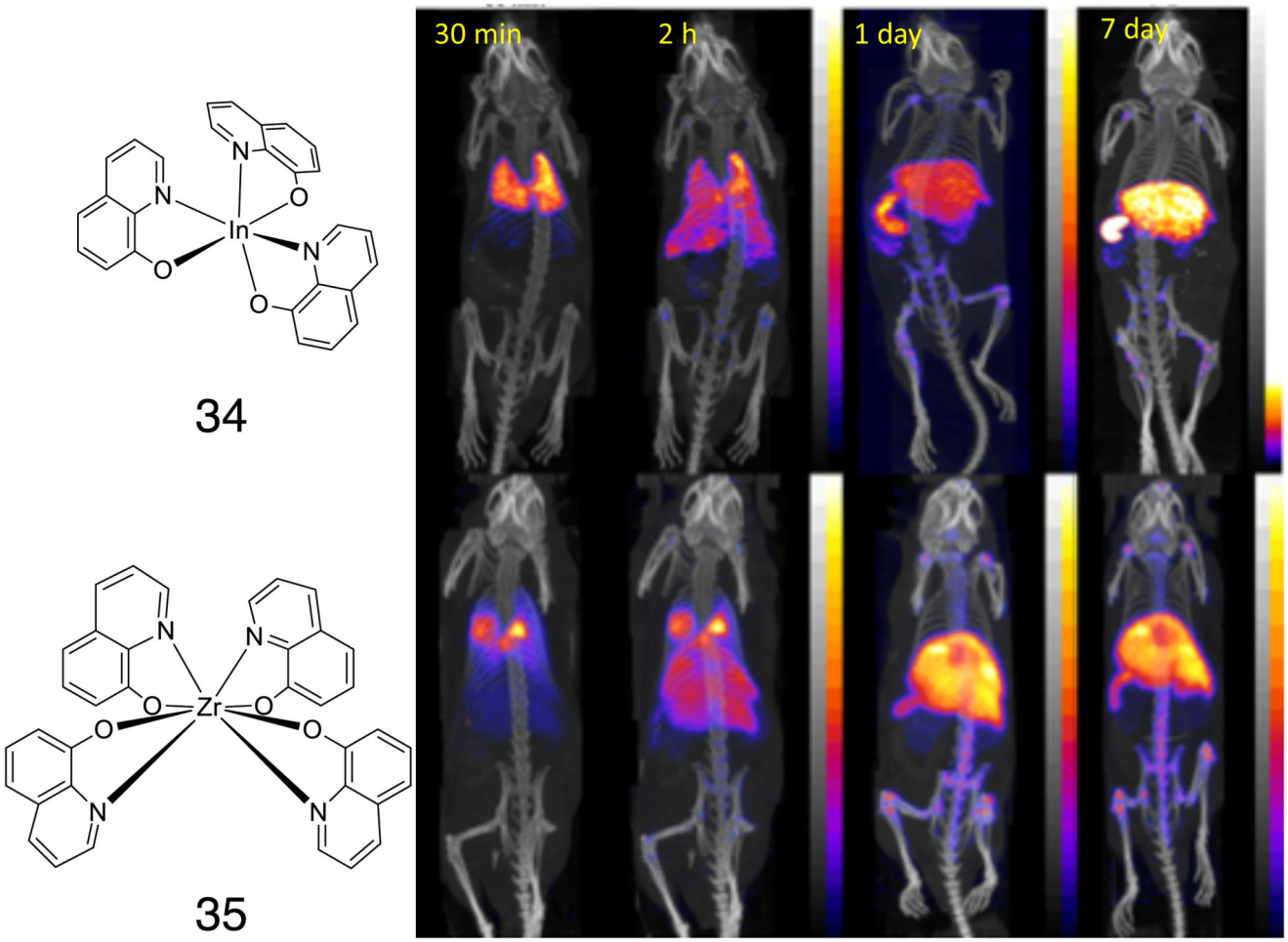

Figure 7.

Left: Complexes of ^{111}In (**34**) and ^{89}Zr (**35**) with 8-hydroxyquinolinate (oxinate); right: time-dependent imaging of myeloma cell migration after intravenous injection of cells labeled with ^{111}In-oxinate and ^{89}Zr-oxinate (SPECT/CT and PET/CT images respectively). Both show broadly similar distribution – initial retention in lungs followed by migration to liver, spleen and bone marrow, but the lower uptake of ^{89}Zr in kidneys compared to ^{111}In in the later images is an indication that the ^{89}Zr shows less efflux from the labeled cells.

Europe PMC Funders Author Manuscripts

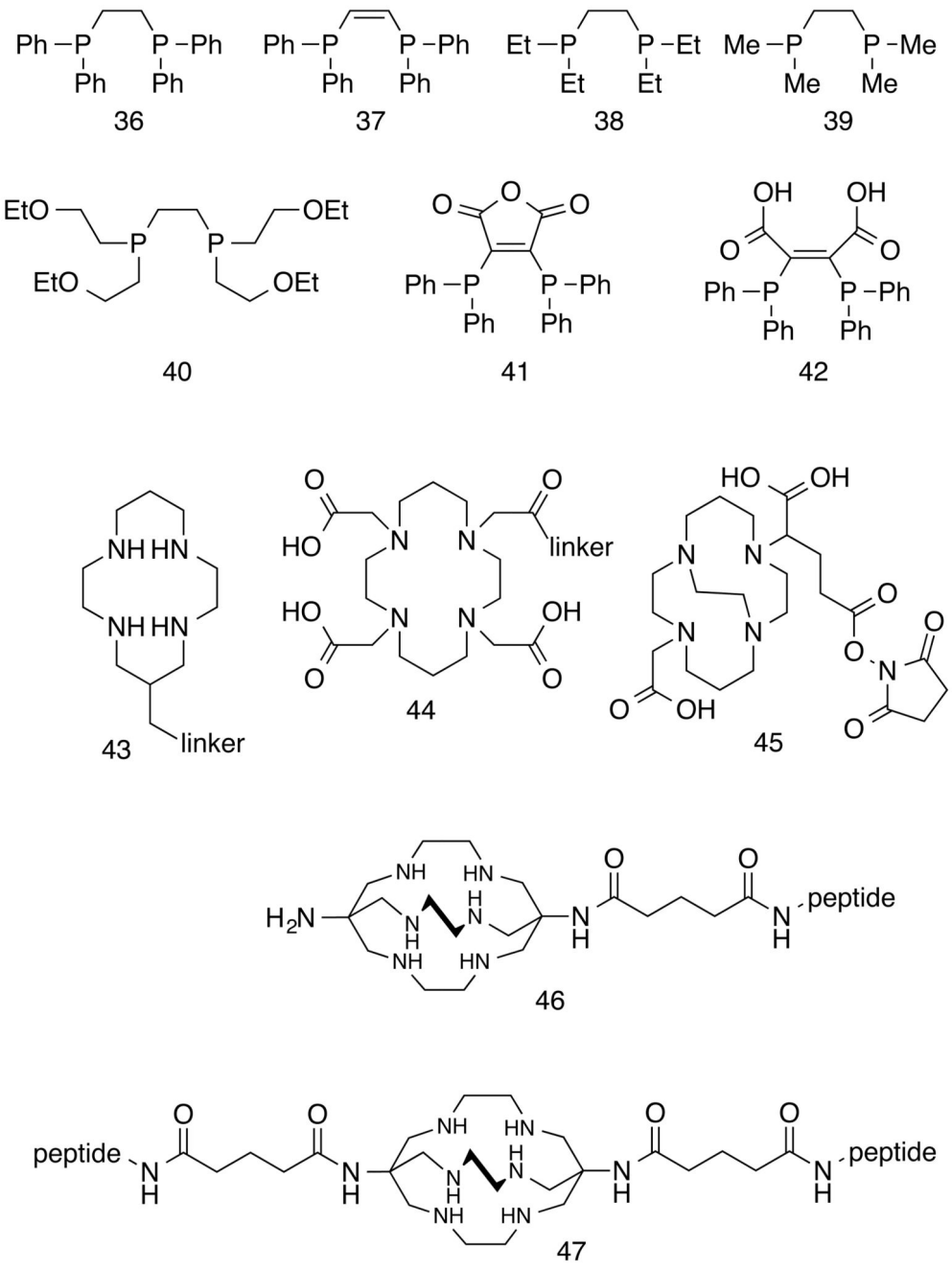

Figure 8.

Chelating agents for copper radionuclides, with copper in oxidation state I (**36** – **42**) and II (**43** – **47**)

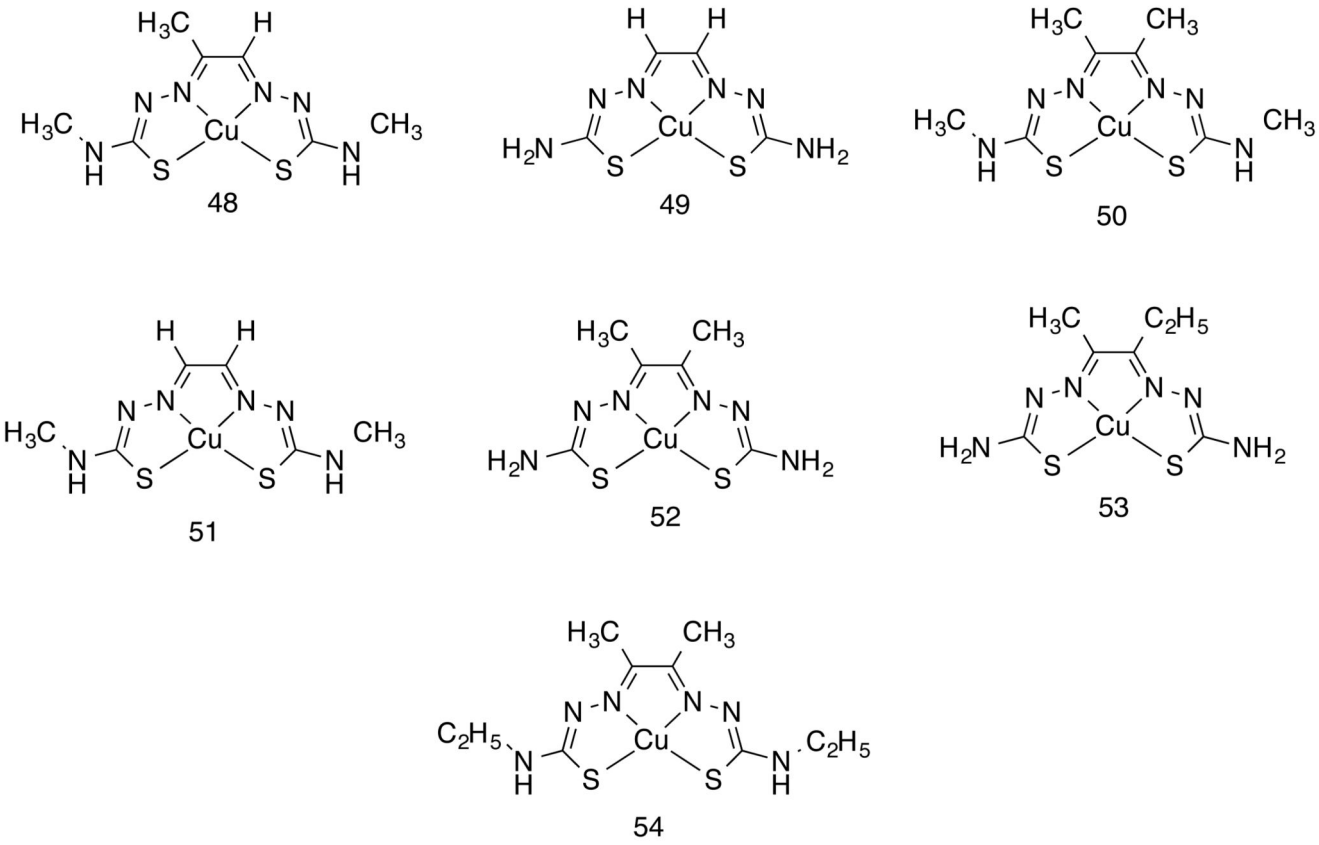

Figure 9.

Bis(thiosemicarbazone) complexes of copper showing variations of structure for control of lipophilicity and control of hypoxia selective and non-selective intracellular trapping.

Europe PMC Funders Author Manuscripts

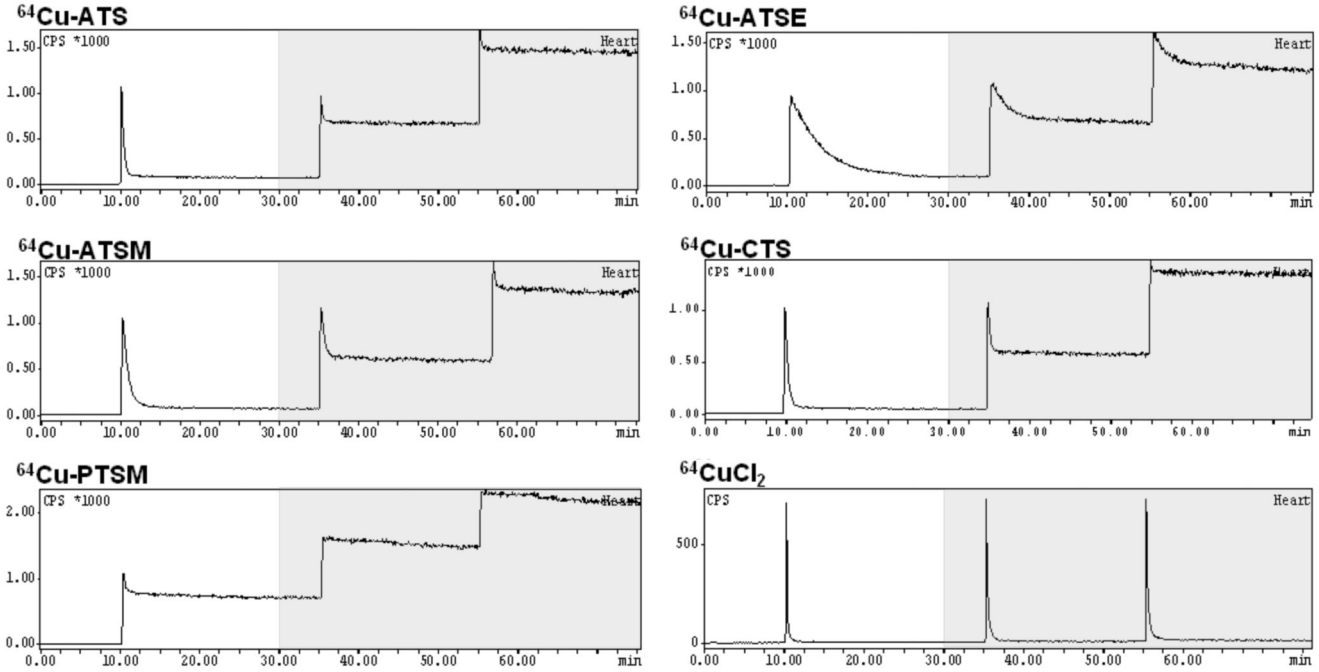

Figure 10.

Time-dependent uptake of radioactivity after injection of a bolus of ^{64}Cu BTSC complexes into isolated Langendorff-perfused rat hearts at 10, 35 and 55 min after the start of perfusion. The y-axis represents radioactivity within the heart. White areas indicate periods of supply of oxygenated buffer while shaded areas indicate supply of anoxic buffer. CuPTSM shows a high level of trapping under oxygenated conditions and even higher (close to 100%) under anoxia). CuATSM on the other hand shows low (ca. 10%) trapping under normoxia increasing to ca. 80% after 25 min hypoxia. CuATS and CuCTS show more rapid transit through the heart than CuATSM, and a greater selectivity in binding to hypoxic compared to normoxic heart. CuATSE (**54**) also shows hypoxia selectivity but takes much longer to transit through the heart because of its increased lipophilicity. Unchelated copper(II) ($CuCl_2$) shows no uptake under either normoxia or hypoxia.

Europe PMC Funders Author Manuscripts

Europe PMC Funders Author Manuscripts

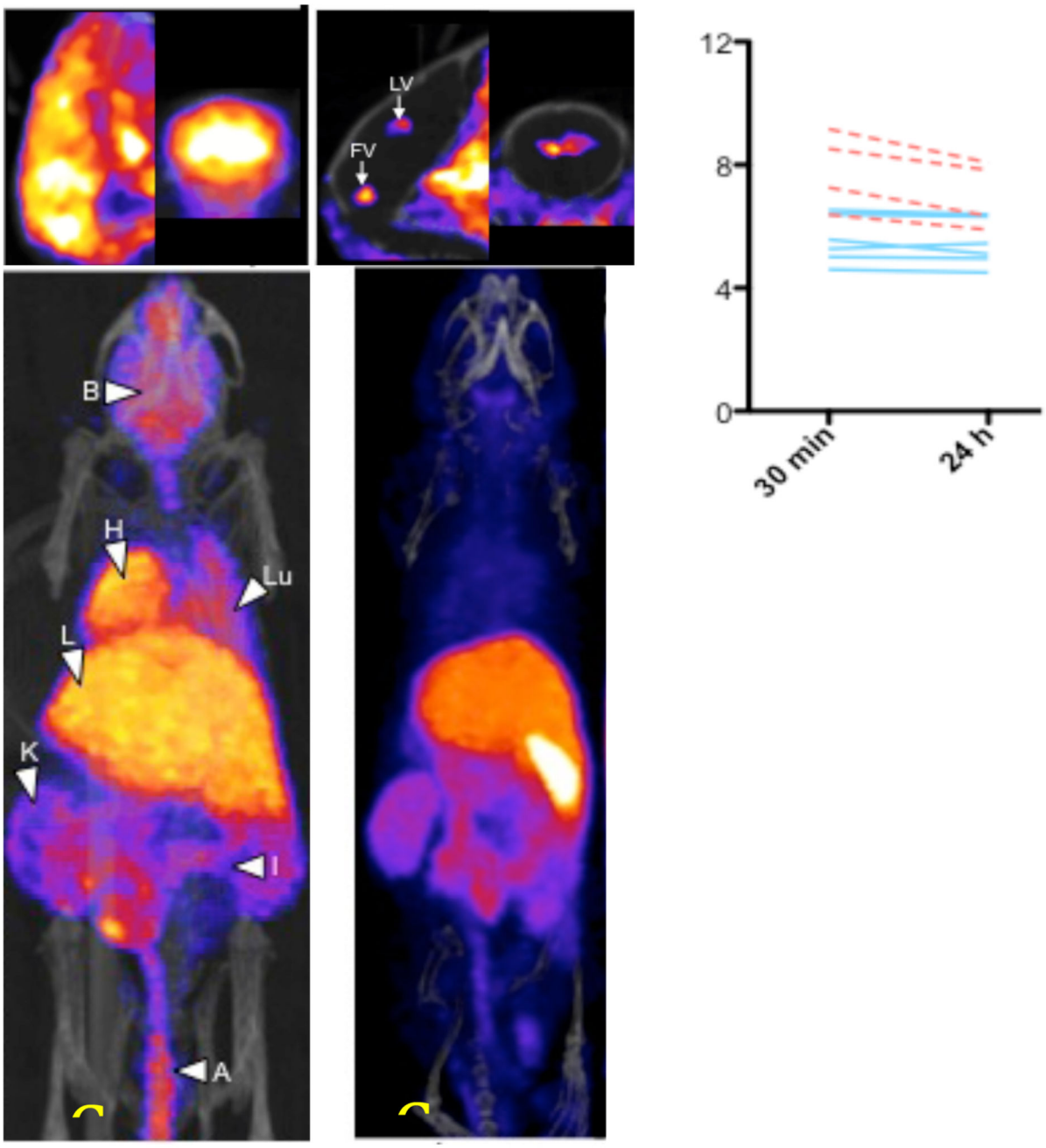

Figure 11.

PET/CT whole body distribution (lower images) of ^{64}Cu in normal mice 30 min after intravenous administration of ^{64}CuGTSM (left) and unchelated (right) ^{64}Cu(II) (acetate salt). The upper images show sagittal and coronal close-ups of the brain showing high global uptake in brain for CuGTSM but focal uptake restricted to the ventricle regions for ionic copper. The graph shows ^{64}Cu concentration 30 min and 24 h after injection of ^{64}CuGTSM in brains of genetically modified mice with Alzheimer's-like pathology (broken lines) with that in their normal counterparts (solid lines).

Europe PMC Funders Author Manuscripts

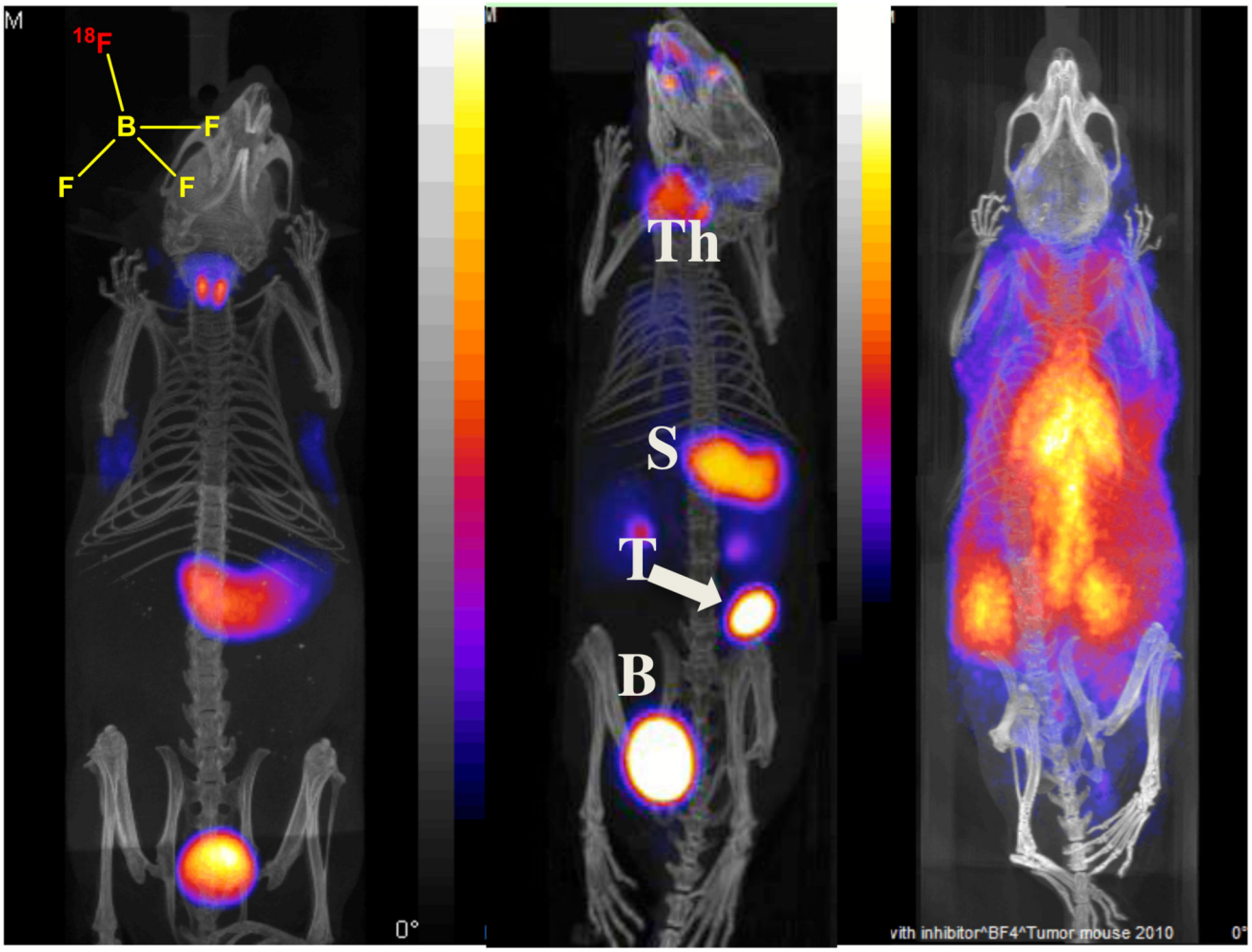

Figure 12.

Biodistribition of ^{18}F-tetrafluoroborate by PET/CT imaging. Left: normal mouse showing thyroid and stomach uptake and excretion into bladder; center: mouse with implanted NIS-expressing breast tumor showing tumor (T) uptake as well as thyroid (Th) and stomach (S) uptake; right: normal mouse pre-injected with perchlorate to block NIS activity, showing radioactivity largely confined to blood pool.

Europe PMC Funders Author Manuscripts

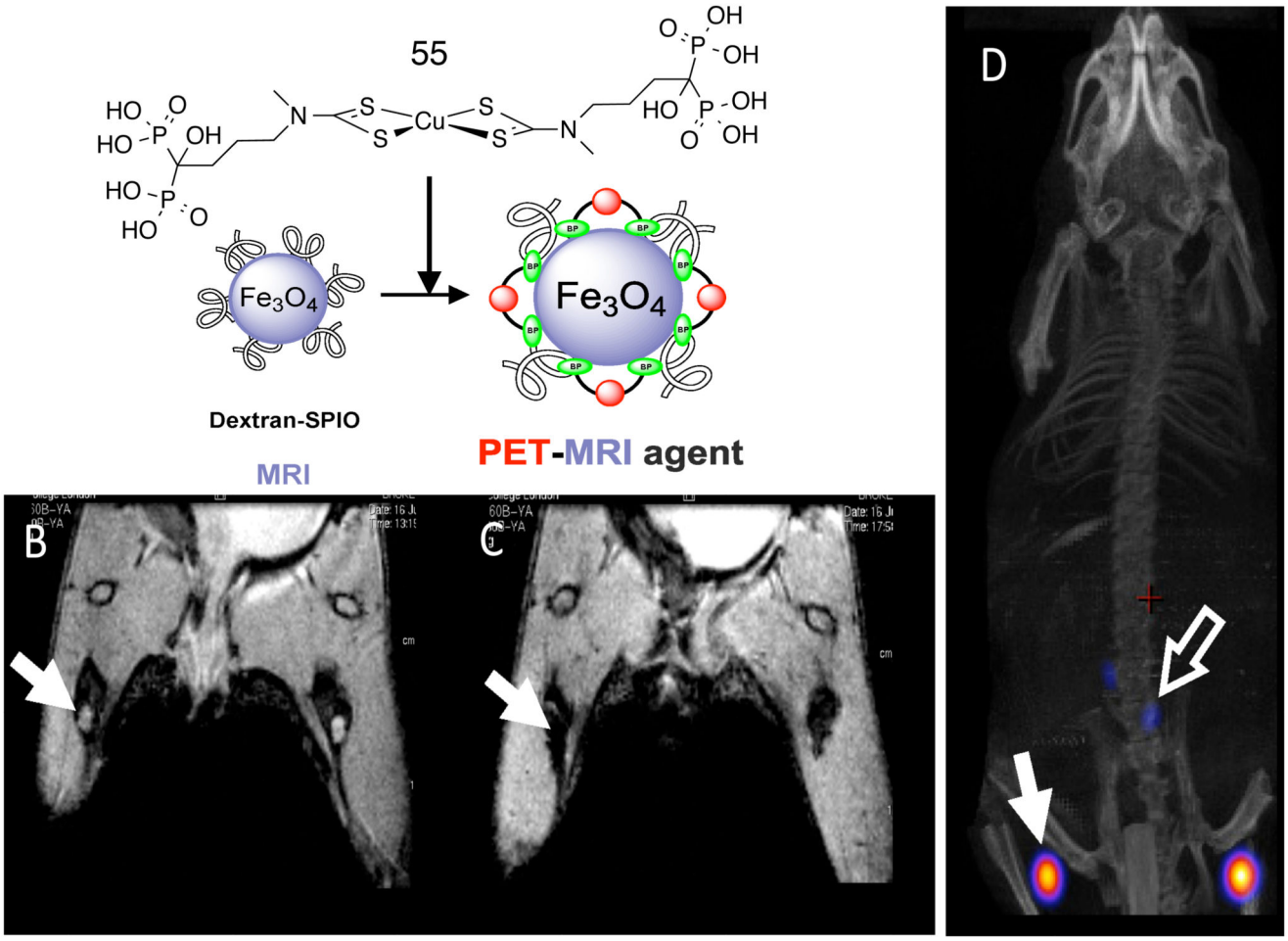

Figure 13.

Top: incorporation of ^{64}Cu into iron oxide nanoparticles exploiting the affinity of copper complexes with pendant bisphosphonate groups (**55**) to the mineral surface. Bottom left: MRI images before (left) and after (right) injection of labeled particles into the footpads of a mouse, showing translocation of particles into lymph nodes indicated by arrows (as identified by loss of signal in the lymph nodes in the right image). On the right is a PET/CT image showing the location of ^{64}Cu in the same lymph nodes as the MRI contrast.